Parametric Optimization of a Double Stage Reheated ORC for Recovering Waste Heat from a Combined Cycle Gas Turbine Power Plant in the Perspective of Repowering

By

Muhammad Reshaeel

00000319863

Session 2019-2021

Supervised by

Dr. Adeel Javed

US-Pakistan Center for Advanced Studies in Energy (USPCAS-E)

National University of Sciences and Technology (NUST)

H-12, Islamabad 44000, Pakistan

Oct 2021

Parametric Optimization of a Double Stage Reheated ORC for Recovering Waste Heat from a Combined Cycle Gas Turbine Power Plant in the Perspective of Repowering

By

Muhammad Reshaeel

00000319863

Session 2019-2021

Supervised by

Dr. Adeel Javed

A Thesis Submitted to the US-Pakistan Center for Advanced Studies in Energy in partial fulfillment of the requirements for the degree of

MASTER of SCIENCE in

THERMAL ENERGY ENGINEERING

US-Pakistan Center for Advanced Studies in Energy (USPCAS-E)

National University of Sciences and Technology (NUST)

H-12, Islamabad 44000, Pakistan

Oct 2021

Thesis Acceptance Certificate

Certified that final copy of MS thesis written by Mr. Muhammad Reshaeel (Registration No. 00000319863), of U.S Pakistan Center for Advanced Studies in Energy has been vetted by undersigned, found complete in all respects as per NUST Statues/Regulations, is within the similarity indices limit and is accepted as partial fulfillment for the award of MS degree. It is further certified that necessary amendments as pointed out by GEC members of the scholar have also been incorporated in the said thesis.

Signature: _____

Name of Supervisor: Dr. Adeel Javed

Date: _____

Signature (HoD): _____

Date: _____

Signature (Dean/Principal): _____

Date: _____

Certificate

This is to certify that work in this thesis has been carried out by **Mr. Muhammad Reshaeel** and completed under my supervision in High Performance Computing laboratory, US-Pakistan Center for Advanced Studies in Energy (USPCAS-E), National University of Sciences and Technology, H-12, Islamabad, Pakistan.

Supervisor: _____

Dr. Adeel Javed
USPCAS-E
NUST, Islamabad

GEC member 1: _____

Dr. Majid Ali
USPCAS-E
NUST, Islamabad

GEC member 2: _____

Dr. Adeel Waqas
USPCAS-E
NUST, Islamabad

GEC member 3: _____

Dr. Mariam Mehmood
USPCAS-E
NUST, Islamabad

HOD-TEE: _____

Dr. Majid Ali
USPCAS-E
NUST, Islamabad

Dean/Principal: _____

Dr. Adeel Waqas
USPCAS-E
NUST, Islamabad

Dedication

Dedicated to those who believed in me and supported me in my journey.

Success takes an investment in time, dedication and sacrifice. This is true education. It is a process.

Acknowledgment

Abstract

The challenge of meeting ever-expanding energy demand and mitigating climate change requires shifting towards renewable technologies while making existing technologies energy-efficient and environment-friendly. The study has conducted multi parametric optimization of a newly modified double stage reheated organic Rankine cycle configuration for the objective function of specific work output and its comparison with other conventional configurations of the organic Rankine cycle for waste heat recovery-based repowering of a degraded combined cycle gas turbine power plant using R245fa, R113, and R141b as the working fluids. Thermodynamic performance of the triple cycle formed by integrating each organic Rankine cycle configuration with the combined cycle gas turbine unit is assessed in terms of repowering, specific fuel consumption and specific water consumption along with the associated greenhouse gas emissions. 24-hour performance variation of the combined cycle gas turbine unit has been incorporated in the analysis. It is found that the double stage reheated organic Rankine cycle configuration has outperformed other configurations in terms of thermodynamic performance. Triple cycle for the double stage reheated organic Rankine cycle has resulted in an average of 1.37% increase in net power output for the working fluid R141b, equivalent to 5.10 MW of additional power output. The thermal efficiency of the triple cycle for double stage reheated organic Rankine cycle has increased by 1.40%, whereas the specific fuel consumption and specific water consumption has reduced by 1.28% and 3.35%, respectively using R141b as the working fluid. The highest waste heat recovery potential is exhibited by the integrated basic organic Rankine cycle configuration for the working fluid R245fa, recovering 30,840 kW of waste heat, equivalent to the burning of 2,467.2 kg/hr of CH_4 and 6784.7 kg/hr CO_2 emissions.

Keywords: Repowering, waste heat recovery, Double stage reheated organic Rankine cycle, Multiparametric optimization, Triple cycle

Table of Contents

List of Figures

List of Tables

List of Publications

1. **ECM-D-21-05399: Parametric Optimization of a Reheated Organic Rankine Cycle and Integration in a Combined Cycle Gas Turbine Power Plant from Triple-Cycle Repowering and Water-Energy Nexus Perspective**

   Energy Conversion and Management (Under review)

   Authors: Muhammad Reshaeel, Adeel Javed, Ahmad Jamil, Majid Ali, Mariam Mahmood, Adeel Waqas

Abbreviations

ORC	Organic Rankine Cycle
CCGT	Combined Cycle Gas Turbine
WHR	Waste Heat Recovery
TC	Triple Cycle
KAPCO	Kot Addu Power Company
BORC	Basic Organic Rankine Cycle
IHE	Internal Heat Exchanger
SRC	Steam Rankine Cycle
DRORC	Double Stage Regenerative Organic Rankine Cycle
ANA	Artificial Neural Network
ABC	Artificial Bees Colony
NSGA-II	Non-Dominated Sorting Genetic Algorithm
GA	Genetic Algorithm
SRORC	Single Stage Regenerative Organic Rankine Cycle
GTC	Gas Turbine Cycle
HRSG	Heat Recovery Steam Generator
GT	Gas Turbine
SFC	Specific Fuel Consumption, kg/kWh
AFS	Annual Fuel Saving, kg
DSRORC	Double Stage Reheated Organic Rankine Cycle
ST	Steam Turbine
EEC	Energy Equation Code
LHV	Lower Heating Value, kg/kWh
TIT	Turbine Inlet Temperature, $^\circ$C
AFSC	Annual Fuel Saving Cost, $
PF	Price of Fuel, $
SWC	Specific Water Consumption, m^3/MWh
HR	Heat Rate, kJ/kWh
ODP	Ozone Depletion Potential
GWP	Global Warming Potential

th   Thermal

a   Air

t   Turbine

p   Pump

s   Supplied

c   Condenser

rh   Reheat

in   Inlet

out   Outlet

CTW   Cooling tower water withdrawn

CTC   Cooling tower water consumed

w   water

mec   Mechanical

isen   isentropic

lat   Latent

cri   Critical

W   Power output, kW

Q   Heat, kW

m   Mass flow rate, kg/s

f   Air to fuel ratio

w   Specific work output, kJ/kg

y   Steam bled fraction from 1st stage

z   Steam bled fraction from 2nd stage

A   Water consumed or withdrawn, m3/MWh

B   Heat utilized in power production and other processes except for cooling kJ/MWh

C   Water required in other processes of a thermal power plant, m3/MWh

Cp   Specific heat, kJ/kg

ΔT Change in temperature, $^{\circ}$ C

hfg   Latent heat of vaporization, kJ/kg

ksen	Fraction of the heat load consumed for sensible heat transfer
ρ	Density, kg/m3
ncc	Number of cycles of concentration
kbd	Fraction of blowdown discharged to the water shed
P	Pressure, kPa
M	Molar Mass, kg/kmol
EJ	Exajoule
s	Entropy, kJ/kg-K
r1	Stage one pressure ratio
q	Specific heat, kJ/kg
η	Efficiency
τ	Annual Operating hours, hr
ε	Effectiveness

Chapter 1 Introduction

1.1 Background

Source: World Energy Council, Paul Scherrer Institute, Accenture Strategy: World Energy Scenarios/2019, September 2019
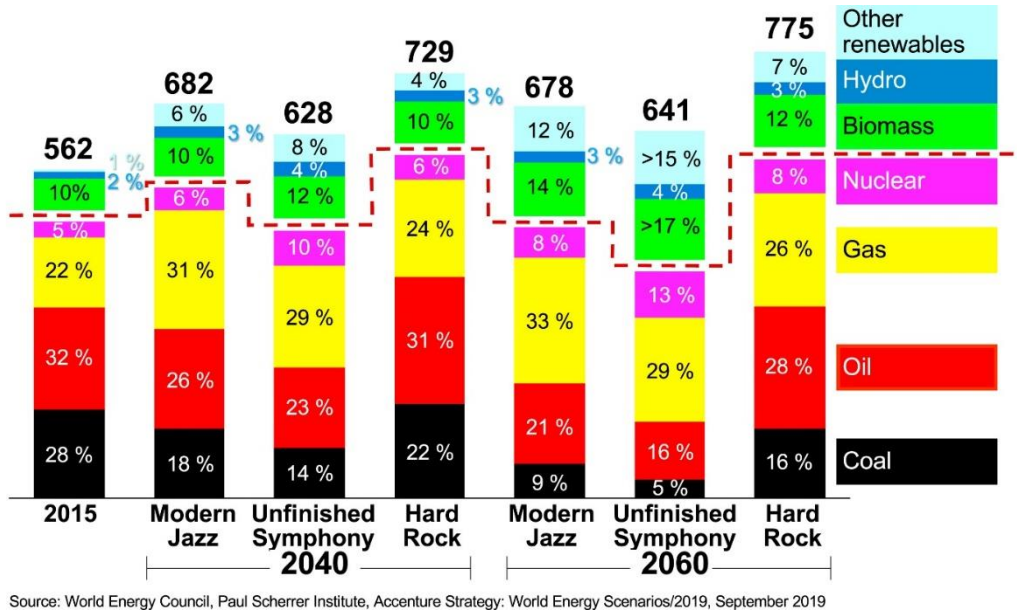
Fig. 1.1 Global energy consumption (primary) and the share of each technology in the future energy mix. Courtesy [3]

The world's demand for primary energy is expected to be in between 800-900 EJ by 2040 [1]. Renewable energy technologies are set to become the prime energy producers yet the global demand for gas is forecasted to increase by 50% by 2040 [2]. As described in Fig. [1.1] the consumption of coal and oil as a primary fuel is going to decline in future but the demand for gas as a fuel will experience a fair increase [3]. The global energy market is facing the challenge of meeting increasing demand while addressing environmental and climate issues. Therefore, considerable measures need to be taken focusing on innovative generation technologies and making existing technologies more efficient with the introduction of improved energy conversion, management, and pollution control techniques [4]. Modern Combined Cycle Gas Turbines (CCGTs) is a reliable technology for generating energy with thermal efficiencies of 60% and higher [5]. They are often termed as a "bridge" towards cleaner and renewable sustainable energy system [6]. Therefore, it is vital to investigate potential cleaner options for enhancing the power generation capacity of CCGTs, which encompasses the introduction of improved waste heat management system for higher efficiency and power output.

1.2   Nature of the issues

The Waste Heat Recovery (WHR) from the exhaust gas of a CCGT holds the potential for repowering the power plant. One of the strategies to achieve this is through converting conventional combined cycle to Triple Cycle (TC) by integrating advanced power cycles. WHR from low to medium grade heat for power generation requires integrating advanced power cycles such as the Kalina cycle [7], Organic Rankine Cycle (ORC) [8], and supercritical CO_2 cycle [9].

In this context, a degraded CCGT power plant owned by the Kot Addu Power Company Ltd. (KAPCO) in Pakistan is considered a case study. The power plant in its degraded state has reduced thermal performance and an exhaust gas temperature in the range of low-grade waste heat. Implementing the TC concept using various ORC configurations presents a repowering opportunity for enhancing thermal efficiency and recovering power output. Along with this, the TC conversion can achieve improved thermal performance with reduced fuel and water consumption and emissions. TC conversion is challenging due to various ORC configurations, working fluid options, and multi-parametric performance indicators. The analysis is further complicated by incorporating 24-hour performance variations and real-time stochastic data of the case study power plant. A complex study like this requires extensive modeling, comparison of available ORC configurations and working fluids, and multi-parametric optimization.

1.3   Scope and objectives of the study

This study conducts parametric optimization of a DSRORC and compares it with other ORC configurations for the optimal thermodynamic parameters. The optimal configurations of the ORC unit are integrated with the CCGT to achieve maximum net power output and waste heat recovery. 24 hr stochastic data of the CCGT unit is incorporated in the analysis of the triple cycle to account for the performance variation of the CCGT. The main objectives of this study are as follows:

a) To model and simulate the CCGT unit in Cycle-Tempo using design data.
b) To model and simulate each ORC configuration in Cycle-Tempo using the heat source data of the CCGT unit.
c) To optimize DSRORC configuration and compare it with other ORC configurations for the optimal thermodynamic parameters.
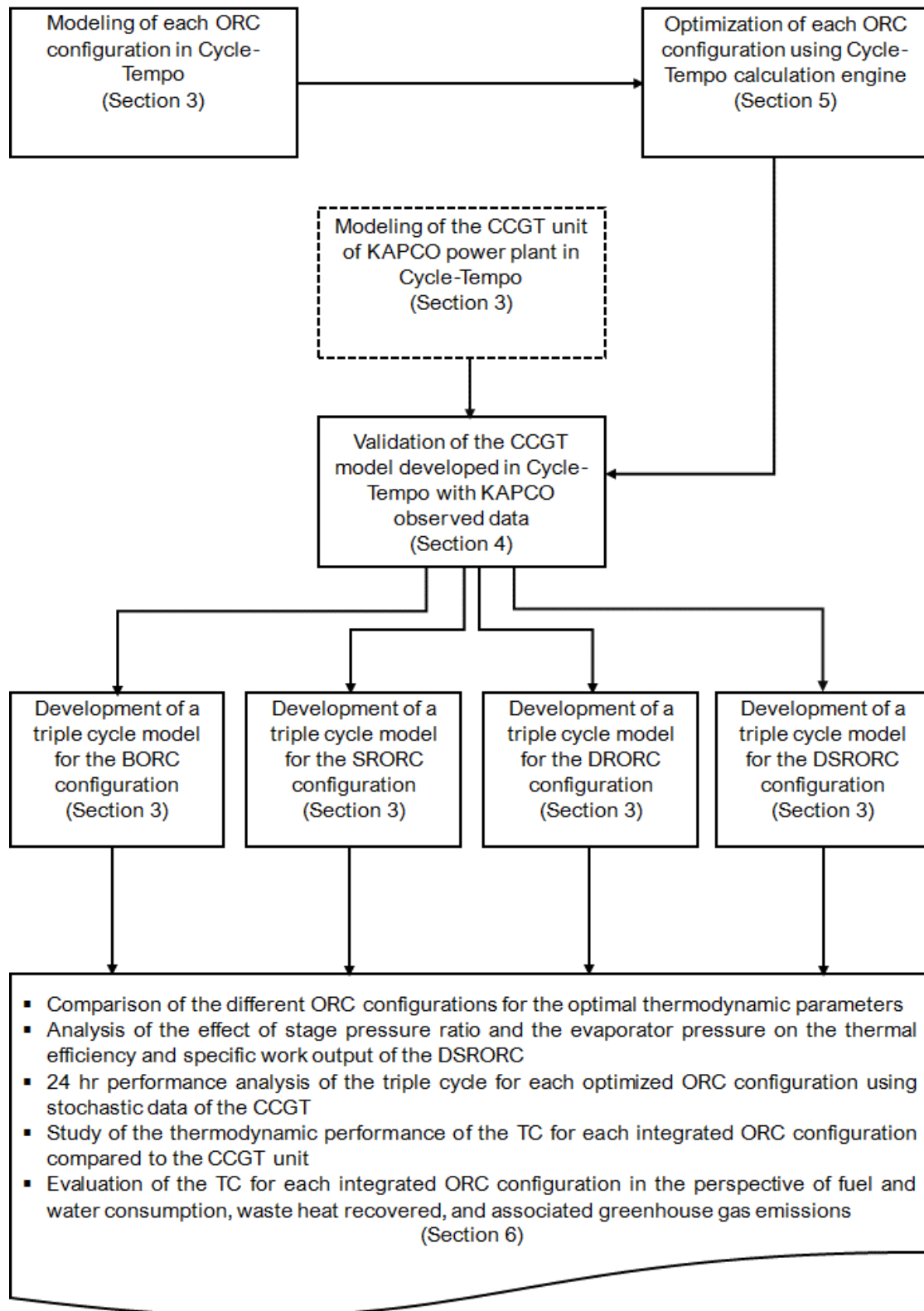
Fig. 1.2 Schematic of the methodology adopted for modeling of the triple cycle and analysis of the impact of each ORC configuration on the performance of triple cycle

3

d) To integrate each ORC configuration with the CCGT using the stochastic data and investigate the performance variation of the triple cycle.

e) To assess the performance of the triple cycle in terms of thermodynamic parameters, fuel-saving, and associated emissions.

Figure 1.2 highlights the methodology adopted in this study.

1.4 Thesis outline

Chapter 1 discusses the energy demand and the share of each technology in the future energy mix. The chapter also emphasizes on how existing technologies needs to be made more energy efficient with better energy conversion technologies to meet the goal of sustainable future. Furthermore, the nature of the issues is discussed, and scope and objectives are defined to cope the issues.

Chapter 2 summarizes the literature reviewed to formulate the methodology and perform the analysis that is aligned with the goals. The different topics covered in the literature review includes the working fluid selection and thermodynamic performance, the comparative analysis and optimization of various ORC configurations using various optimization techniques. Finally, the application of ORC for WHR is elaborated and the literature gap is identified which signifies the need of this work.

The KAPCO powerplant and the TC model is described for each ORC configuration integrated with the CCGT unit of the energy block -1A of the facility. A complete schematic layout of the facility and each ORC configuration along with the Ts- diagrams are elaborated and discussed in detail in this chapter. The basic working of each ORC configuration for the TC and the basic process involved in the thermodynamic modeling of the system is also a matter of subject in this chapter.

Chapter 4 deals with the mathematical model and the calculation engine of Cycle-Tempo that is responsible for modeling the system and obtaining relevant results. The chapter discusses the basic working of Cycle-Tempo for performing thermodynamic analysis of the respective cycles. The chapters also laid the foundation of the mathematical model employed to evaluate the thermodynamic performance of the system along with the calculation of SFC, SWC and emissions.

The results obtained from the mathematical model developed and explained in chapter 4 are discussed and represented in chapter 5.

Chapter 6 summarizes the work that is conducted in this study. The challenges that were faced during the research are also highlighted. Future work that can be done related to this study is also discussed.

Summary

The world's energy demand is increasing exponentially. To achieve the goal of a sustainable future with zero or negative net carbon emissions in true essence, it is necessary to switch towards renewable energy generation technologies while making existing technologies superior that are more energy efficient with lesser emissions. CCGT is considered as a bridge technology towards a cleaner and sustainable energy system, therefore it is pivotal to discover potential options for repowering the CCGTs in a manner that its thermal efficiency is also enhanced while emissions are reduced. In this perspective, an ORC unit is integrated with a CCGT unit of Pakistan's based power generation facility called KAPCO to form a triple cycle. Stochastic data of the CCGT unit is incorporated in the analysis to incorporate the variations in net power output. A novel configuration of ORC unit that is DSRORC is parametrically optimized and compared with the other ORC configurations for the optimal thermodynamic parameters and thermodynamic analysis of the triple cycle is carried out in the perspective of net power output, thermal efficiency, specific fuel consumption, specific water consumption and emissions.

References

[1]   Skea J, van Diemen R, Portugal-Pereira J, Khourdajie A Al. Outlooks, explorations and normative scenarios: Approaches to global energy futures compared. Technol Forecast SocChange2021;168:120736.https://doi.org/https://doi.org/10.1016/j.techfore.2021.120736.

[2]   Ahmad T, Zhang D. A critical review of comparative global historical energy consumption and future demand: The story told so far. Energy Reports 2020;6:1973–91. https://doi.org/https://doi.org/10.1016/j.egyr.2020.07.020.

[3]   Kober T, Schiffer H-W, Densing M, Panos E. Global energy perspectives to 2060 – WEC's World Energy Scenarios 2019. Energy Strateg Rev 2020;31:100523. https://doi.org/https://doi.org/10.1016/j.esr.2020.100523.

[4]   Mahmoudi A, Fazli M, Morad MR. A recent review of waste heat recovery by Organic Rankine Cycle. Appl Therm Eng 2018;143:660–75.https://doi.org/https://doi.org/10.1016/j.applthermal eng.2018.07.136.

[5]   Woudstra N, Woudstra T, Pirone A, Van der Stelt T. Thermodynamic evaluation of combined cycle plants. Energy Convers Manag 2010;51:1099–110. https://doi.org/10.1016/j.enco nman.2009.12.016.

[6]   Carapellucci R, Giordano L. Regenerative gas turbines and steam injection for repowering combined cycle power plants: Design and part-load performance. Energy Convers Manag 2021;227:113519. https://doi.org/https://doi.org/10.1016/j.enconman.2020.113519.

[7]   Júnior EPB, Arrieta MDP, Arrieta FRP, Silva CHF. Assessment of a Kalina cycle for waste heat recovery in the cement industry. Appl Therm Eng 2019;147:421–37. https://doi.org/https://doi.org/10.1016/j.applthermaleng.2018.10.088.

[8]   Aliahmadi M, Moosavi A, Sadrhosseini H. Multi-objective optimization of regenerative ORC system integrated with thermoelectric generators for low-temperature waste heat recovery. Energy Reports 2021;7:300–13. https://doi.org/https://doi.org/10.1016/j.egyr.202 0.12.035.

[9]   Kim YM, Sohn JL, Yoon ES. Supercritical CO2 Rankine cycles for waste heat recovery from gas turbine. Energy 2017;118:893–905. https://doi.org/https://doi.org/10.1016/j.ene rgy.2016.10.106.

Chapter 2 Literature Review

2.1 Prolegomenon

CCGT is a premium power generation technology, and the focus is to improve its thermodynamic performance while keep the emissions minimum. Various repowering techniques have been proposed to improve the thermodynamic efficiency and net power output of the CCGT but to achieve the goal zero or negative carbon emissions such technologies must be proposed that increases the net power output while reducing the overall emissions. ORC is one such technology that is excellent for recovering waste heat, improving thermal efficiency and providing increased net power output while reducing the emissions. The work that has been done so far on ORC can be classified into working fluid and cycle configuration selection, parametric and sensitivity analysis, optimization, sizing and selection of the appropriate turbomachinery and technoeconomic analysis.

2.2 Analysis of different ORC configurations for different working fluid types and optimization techniques

The work that has been done so far on ORC is interdependent and integrated. Therefore, it is necessary to correlate and understand the ORC technology in the unison of working fluid and configuration selection and the optimization techniques adopted to analyze the thermodynamic performance.

2.2.1 Performance analysis of different ORC configurations

Various cycle configurations have been developed for the ORC and have been investigated for various operating parameters. Sensitivity analysis conducted by Xi et al. [1] on the Basic ORC (BORC) and regenerative ORC described the inlet expander turbine as a crucial factor in determining thermal efficiency and power output. Lecompte et al. [2] critically reviewed different ORC configurations with the identification of their challenges. Li [3] concluded that for constant net power output, the thermal efficiency of a reheated ORC was closed to a BORC, whereas regenerative ORC and ORC with an Internal Heat Exchanger (IHE) had higher thermal efficiencies than BORC due to lower evaporator load. Optimization and comparative analysis of a recuperative and regenerative ORC, performed by K.Braimakis et al. [4] showed that simple recuperative ORC had higher thermal efficiency than regenerative ORC. Recuperative ORC with a closed feedwater heater resulted in a 6.22% to 9.22% increase in thermal efficiency

than simple recuperative ORC. Goodarzi et al. [5] analyzed a reheated ORC and found that the introduction of reheat between the turbine stages led to improved thermal efficiencies. Zhang et al. [6] conducted a comparative analysis between a Steam Rankine Cycle (SRC), an ORC, and steam-organic Rankine cycle. The results suggested that ORC was more efficient for the low-temperature heat source than the SRC, whereas the steam-organic Rankine cycle had a better profile matching with the heat source temperature.

2.2.2 Working fluid selection and performance analysis

In the context of the performance and selection of working fluids, several studies have been documented. In the thermodynamic performance assessment of different working fluids conducted by Tchanche et al. [7], it was found out that R134a followed by R152a, R600, R600a, and R290 was the most appropriate candidates for the low-temperature heat source. Zhang et al. [8] evaluated the performance of dry and isentropic working fluids and established selection criteria based on pump performance for a small-scale ORC. A techno-economic study carried out by Andreasen et al. [9] suggested that the techno-economic advantages of using zeotropic mixtures over pure working fluids were more sensitive to variations in the electricity cost, working fluid cost, and models for cost estimation of equipment. Liu et al. [10] studied WHR from a geothermal heat source for varying temperatures using a pure 600a/R601a mixture. Net power output increments of 11%, 7%, and 4% were observed for the heat source temperatures of 110 ℃, 130 ℃ and, 150 ℃, respectively. Parametric optimization of the ORC was used to classify the working fluids based on superheater pressure by A.Fernandez et al. [11] .It was found that fluids with lower working pressures and higher turbine inlet temperatures resulted in higher thermal efficiency.

2.2.3 Optimization techniques

Different optimization techniques are employed for the parametric optimization of the ORC. Double Stage Regenerative ORC (DRORC) was optimized for the objective function of thermal efficiency, exergy efficiency and specific work using Artificial Neural Network (ANA), and Artificial Bees Colony (ABC) method by Rashidi et al. [12]. Imran et al. [13] used Non-Dominated Sorting Genetic Algorithm (NSGA-II) for the parametric optimization of different configurations of ORC. An increase of 1.01% and 1.45% in thermal efficiency was observed while changing from BORC to single and dual-stage regenerative ORC, respectively. Pierobon et al. [14] used Genetic Algorithm (GA) to perform multi-objective optimization of a MW-size ORC for the objective function of thermal efficiency, the total volume of the

system, and net present value in an offshore application. An identical study by Wang et al. [15], used GA for multi-objective optimization of two contrasting objective functions: exergy efficiency and overall capital cost.

2.2.4 Thermodynamic performance assessment of ORC configurations using different optimization techniques

Studies on thermodynamic optimization, working fluid selection, and cycle configuration are interrelated. Laouid et al. [16] performed dual-objective optimization for a regenerative ORC and ORC with IHE using 12 different working fluids. The study revealed that the selection of net power output and electrical production cost as the objective function led to better utilization of exhaust gas thermal energy and lower electrical production cost for all the fluids studied. A similar study was conducted by Walraven et al. [17] using 80 different working fluids for sub-critical, trans-critical and multi-pressure ORC with a comparative analysis between these configurations and the Kalina cycle. Wang et al. [18] proposed a novel criteria for ORC fluid selection in a dual-loop ORC for WHR of an engine exhaust using multi-objective optimization. Among the 24 working fluids analyzed, toluene/R124 showed the best thermal performance. It was also found that critical temperature was a key parameter for pairs of working fluids compared to boiling point due to its unique characteristics. Similarly, Xia et al. [19] proposed a novel evaluation scheme using the grey relational method to select optimal cycle parameters and working fluids. Six different working fluids were analyzed, and butane was classified as the lowest global warming potential working fluid whereas, R1234yf was more appropriate when the exhaust gas temperature was lower than 170 °C. A regenerative ORC was parametrically optimized for the subcritical, superheated subcritical, and transcritical configuration using 14 different working fluids by Javanshir et al. [20]. Results indicated that working fluids with high specific heats tend to have higher specific work output, whereas working fluids having higher critical temperature produces higher thermal efficiency. Xi et al. [21] performed the parametric optimization of a regenerative ORC using GA. Results indicated that the DRORC outperforms Single Stage Regenerative ORC (SRORC) and BORC in terms of thermal efficiency.

2.3 Applications of ORC for recovering waste heat

ORC technology has widespread applications and can recover waste heat from a variety of heat sources. Kalina cycle and ORC were compared for recovering waste heat from a diesel engine by Bombarda et al. [22]. The conversion of low-grade waste heat into power using the ORC

for various applications was studied by Tchanche et al. [23]. A comparative analysis between the Kalina cycle and ORC for a multi-stream WHR was performed by Wang et al. [24]. The dynamic model of an ORC for WHR from a diesel engine was developed by Huster et al. [25]. Optimization of ORC for the WHR of an internal combustion engine for the objective function of exergy efficiency and net power output was performed by Seyedkavoosi et al. [26]. Multi-objective optimization and the exergy analysis of an ORC system for WHR of a Brazilian floating product storage offload was performed by T.Gotelip et al. [27]. The analysis conducted by A.Surendran et al. [28] showed that for dual-source waste heat, series two-stage ORC delivered 8.5% more net power output than single-stage pre-heated ORC, while parallel two-stage ORC resulted in 0.3% less net power output. Lim et al. [29] conducted a thermo-economic evaluation and optimum working fluid selection analysis of a double stage ORC and an added double stage ORC for WHR from a liquified natural gas-fueled ship. Carcazi et al. [30] analyzed the WHR system of an aero-derivative Gas Turbine Cycle (GTC) exhaust and its intercooler. Emadi et al. [31] performed the multi-objective optimization of a dual-loop ORC system for a solid oxide fuel cell WHR system using GA and neural network method. It was found that R601 in the top and ethane in the bottom loop of the ORC enabled the optimal trade-off between exergy efficiency and capital cost. Lin et al. [32] investigated the experimental performance of a 10 kW ORC system, highlighting that the degree of superheating and expander pressure ratio had a significant effect on thermal efficiency.

2.4 Performance enhancement of CCGT

A Significant amount of research has been done on improving the thermodynamic performance of the CCGT. A Study conducted by Srinivas et al. [33] revealed that thermal efficiency of the CCGT system increased by converting single pressure Heat Recovery Steam Generator (HRSG) to double and triple pressure HRSG at the expense of system complexity and HRSG cost. Carapellucci et al. [34] considered the prospect of repowering a CCGT power plant by injecting steam produced by the feed of an additional turbine which resulted in enhanced power output and operating flexibility without significant efficiency penalty. Carapellucci et al. [35] proposed a novel method to repower a CCGT using regenerative gas turbine and steam injection.

2.5 Triple cycle performance analysis

Several studies have been documented on the integration of ORC with the CCGT unit. Roy et al. [36] concluded that the integration of ORC with the power plants resulted in reduced emissions, enhanced thermal efficiency, and reduced power burden. A study conducted by Srinivas et al. [37] on the integration of ORC with the CCGT to form TC revealed that a parallel combination of ORC and SRC with a Gas Turbine (GT) unit had superior thermodynamic performance than the series combination of ORC and SRC The experimental results of a study conducted by Qui et al. [38] indicated that for combined heat and power application, ORC resulted in increased energy efficiency with a thermal output of 14 kW and an electrical power output of 0.65 kW. Kose et al. [39] performed the parametric optimization of an SRC and ORC integrated with the GT for the varying turbine inlet pressure, and temperature Results showed that among the different working fluids analyzed, r141b performed the best, and a total of 9136 kW of waste heat corresponding to the burning 734 kg/h of natural gas, comparable to 2203.73 CO_2 kg/h emissions was recovered. A similar study conducted by Sachdeva et al. [40] showed that a solar-powered TC resulted in improved thermodynamic performance and zero carbon emissions. WHR system developed and optimized for a 600 MW power plant by Shamsi et al. [41], resulted in 6 MW of additional power output in case of a water-cooled condenser and 3.9 MW in case of an air-cooled condenser. Analysis carried by Balanesscu et al. [42] on the integration of ORC with the gas steam combined cycle indicated that its thermal efficiency increased by 1.1% with reduced Specific Fuel Consumption (SFC) and increased Annual Fuel Saving (AFS). Hemadri et al. [43] investigated the effect of reheat on the combined cycle performance in the perspective of repowering and reported that specific thermal work output increased by incorporating reheat in the ORC.

2.6 Research gap recognition and significance of the work

Detailed literature review reveals that the work done so far on the TC conversions of CCGTs considers the integration of a single ORC configuration only. This study investigates the integration, performance and optimization of a modified ORC with a degraded CCGT power plant for repowering. The modified configuration is a Double Stage Reheated ORC (DSRORC) that lacks detailed investigation for WHR based repowering. The DSRORC is modeled for three working fluids, namely R245fa, R113, and R141b, and is compared with the configurations of BORC, SRORC, and DRORC for the same repowering application. Furthermore, this study utilizes a CCGT modeled using real-time performance data with

uncertainties investigated by Jamil et al [44] as an extension of their work The TC integration is assessed in terms of thermal performance, SFC, Specific Water Consumption (SWC) and emissions, along with the comparative thermal analysis of the ORC configurations. The incorporation of 24-hour performance variations of the CCGT increase the complexity of this study, making it a valuable addition to the body of knowledge on WHR based applications of ORCs.

Summary

This chapter summarizes the work that has been done relevant to the topic under consideration. The research that is already carried out on the relevant topic is categorized into selection and thermodynamic performance of the working fluid, parametric optimization using different optimization techniques, technoeconomic analysis and configuration analysis. The work is integrated and usually interdependent. Furthermore, the scope of ORC and its applications are discussed, particularly the application of ORC to recover waste heat from CCGT forming **TC** is highlighted. The detailed literature review has enabled to realize the gap in the work that has been done on ORC so far for recovering waste heat from CCGT. This also strengthened the work that is carried out in this study.

References

[1]   Xi H, Zhang H, He Y-L, Huang Z. Sensitivity analysis of operation parameters on the system performance of organic Rankine cycle system using orthogonal experiment. Energy 2019;172:435–42. https://doi.org/https://doi.org/10.1016/j.energy.2019.01.072.

[2]   Lecompte S, Huisseune H, van den Broek M, Vanslambrouck B, De Paepe M. Review of organic Rankine cycle (ORC) architectures for waste heat recovery. Renew Sustain Energy Rev 2015;47:448–61. https://doi.org/https://doi.org/10.1016/j.rser.2015.03.089.

[3]   Li G. Organic Rankine cycle performance evaluation and thermoeconomic assessment with various applications part I: Energy and exergy performance evaluation. Renew Sustain Energy Rev 2016;53:477–99.https://doi.org/https://doi.org/10.1016/j.rser.2015.08.066.

[4]   Braimakis K, Karellas S. Energetic optimization of regenerative Organic Rankine Cycle configurations. Energy Convers Manag 2018;159:35370.https://doi.org/https://doi.org/10.1016/j.enconman.2017.12.093.

[5]   Goodarzi M, Soltani HD. Thermal performance analysis of a reheating-regenerative organic Rankine cycle using different working fluids. Mechanika 2015;21:28–33. https://doi.org/10.5755/j01.mech.21.1.10127.

[6]   Zhang X, Wu L, Wang X, Ju G. Comparative study of waste heat steam SRC, ORC and S-ORC power generation systems in medium-low temperature. Appl Therm Eng 2016;106:1427–39. https://doi.org/https://doi.org/10.1016/j.applthermaleng.2016.06.108.

[7]   Tchanche BF, Papadakis G, Lambrinos G, Frangoudakis A. Fluid selection for a low-temperature solar organic Rankine cycle. Appl Therm Eng 2009;29:2468–76. https://doi.org/https://doi.org/10.1016/j.applthermaleng.2008.12.025.

[8]   Zhang X, Zhang Y, Wang J. Evaluation and selection of dry and isentropic working fluids based on their pump performance in small-scale organic Rankine cycle. Appl Therm Eng 2021;191:116919. https://doi.org/https://doi.org/10.1016/j.applthermaleng.2021.116919.

[9]   Andreasen JG, Baldasso E, Kærn MR, Weith T, Heberle F, Brüggemann D, et al. Techno-economic feasibility analysis of zeotropic mixtures and pure fluids for organic Rankine cycle systems. Appl Therm Eng 2021;192:116791. https://doi.org/https:// doi.org/10.1016 /j.applthermal eng.2021.116791.

[10]   Liu Q, Shen A, Duan Y. Parametric optimization and performance analyses of geothermal organic Rankine cycles using R600a/R601a mixtures as working fluids. Appl Energy 2015;148:410–20. https://doi.org/https://doi.org/10.1016/j.apenergy.2015.03.093.

[11]   Fernández-Guillamón A, Molina-García Á, Vera-García F, Almendros-Ibáñez JA. Organic Rankine Cycle Optimization Performance Analysis Based on Super-Heater Pressure: Comparison of Working Fluids. Energies 2021;14. https://doi.org/10.3390/en14092548.

[12]   Rashidi MM, Galanis N, Nazari F, Basiri Parsa A, Shamekhi L. Parametric analysis and optimization of regenerative Clausius and organic Rankine cycles with two feedwater heaters using artificial bees colony and artificial neural network. Energy 2011;36:5728–40. https://doi.org/10.1016/j.energy.2011.06.036.

[13]   Imran M, Park BS, Kim H, Lee DH, Usman M, Heo M. Thermo-economic optimization of Regenerative Organic Rankine Cycle for waste heat recovery applications. Energy Convers Manag 2014;87:107–118. https://doi.org/10.1016/j.enconman.2014.06.091.

[14]   Pierobon L, Nguyen T-V, Larsen U, Haglind F, Elmegaard B. Multi-objective optimization of organic Rankine cycles for waste heat recovery: Application in an offshore platform. Energy 2013;58:538–49. https://doi.org/https://doi.org/10.1016/j.energy.2013.05.039.

[15]   Wang J, Yan Z, Wang M, Li M, Dai Y. Multi-objective optimization of an organic Rankine cycle (ORC) for low grade waste heat recovery using evolutionary algorithm. Energy Convers Manag 2013;71:146–58 https://doi.org/https://doi.org/10.1016/j.enconman.2013.03.028.

[16]   Laouid YAA, Kezrane C, Lasbet Y, Pesyridis A. Towards improvement of waste heat recovery systems: A multi-objective optimization of different organic Rankine cycle configurations. International Journal of Thermofluids 2021;11:100100. https://doi.org/https://doi.org/10.1016/j.ijft.2021.100100.

[17]   Walraven D, Laenen B, D'haeseleer W. Comparison of thermodynamic cycles for power production from low-temperature geothermal heat sources. Energy Convers Manag 2013;66:220–33. https://doi.org/https://doi.org/10.1016/j.enconman.2012.10.003.

[18]   Wang Z, Hu Y, Xia X, Zuo Q, Zhao B, Li Z. Thermo-economic selection criteria of working fluid used in dual-loop ORC for engine waste heat recovery by multi-objective

optimization. Energy 2020;197:117053. https://doi.org/https://doi .org/10.1016/j.energy.2020. 117053.

[19]   Xia XX, Wang ZQ, Hu YH, Zhou NJ. A novel comprehensive evaluation methodology of organic Rankine cycle for parameters design and working fluid selection. Appl Therm Eng 2018;143:283–92. https://doi.org/https://doi.org/10.1016/j.applthermaleng.2018.07.061.

[20]   Javanshir A, Sarunac N, Razzaghpanah Z. Thermodynamic analysis of a regenerative organic Rankine cycle using dry fluids. Appl Therm Eng 2017;123:852–64. https://doi.org /https://doi.org/10.1016/j.applthermaleng.2017.05.158.

[21]   Xi H, Li M-J, Xu C, He Y-L. Parametric optimization of regenerative organic Rankine cycle (ORC) for low grade waste heat recovery using genetic algorithm. Energy 2013;58:473– 82. https://doi.org/https://doi.org/10.1016/j.energy.2013.06.039.

[22]   Bombarda P, Invernizzi CM, Pietra C. Heat recovery from Diesel engines: A thermodynamic comparison between Kalina and ORC cycles. Appl Therm Eng 2010;30:212– 9. https://doi.org/https://doi.org/10.1016/j.applthermaleng.2009.08.006.

[23]   Tchanche BF, Lambrinos G, Frangoudakis A, Papadakis G. Low-grade heat conversion into power using organic Rankine cycles – A review of various applications. Renew Sustain Energy Rev 2011;15:3963–79. https://doi.org/https://doi.org/10.1016/j.rser.2011.07.024.

[24]   Wang Y, Tang Q, Wang M, Feng X. Thermodynamic performance comparison between ORC and Kalina cycles for multi-stream waste heat recovery. Energy Convers Manag 2017;143:482–92. https://doi.org/https://doi.org/10.1016/j.enconman.2017.04.026.

[25]   Huster WR, Vaupel Y, Mhamdi A, Mitsos A. Validated dynamic model of an organic Rankine cycle (ORC) for waste heat recovery in a diesel truck. Energy 2018;151:647–61. https://doi.org/https://doi.org/10.1016/j.energy.2018.03.058.

[26]   Seyedkavoosi S, Javan S, Kota K. Exergy-based optimization of an organic Rankine cycle (ORC) for waste heat recovery from an internal combustion engine (ICE). Appl Therm Eng 2017;126:447–57. https://doi.org/https://doi.org/10.1016/j.applthermaleng.2017.07.124.

[27]   Gotelip Correa Veloso T, Sotomonte CAR, Coronado CJR, Nascimento MAR. Multi-objective optimization and exergetic analysis of a low-grade waste heat recovery ORC

application on a Brazilian FPSO. Energy Convers Manag 2018;174:537–51.https://doi .org/https://doi.org/10.1016/j.enconman.2018.08.042.

[28]   Surendran A, Seshadri S. Performance investigation of two stage Organic Rankine Cycle (ORC) architectures using induction turbine layouts in dual source waste heat recovery. Energy Convers Manag X 2020;6:100029. https://doi.org/https:// doi.org/10.1016/j.ecmx.2020 . 100029.

[29]   Lim T-W, Choi Y-S, Hwang D-H. Optimal working fluids and economic estimation for both double stage organic Rankine cycle and added double stage organic Rankine cycle used for waste heat recovery from liquefied natural gas fueled ships. Energy Convers Manag:2021;242:114323. https://doi.org/https://doi.org/10.1016/j.enconman.2021.114323.

[30]   Carcasci C, Winchler L. Thermodynamic Analysis of an Organic Rankine Cycle for Waste Heat Recovery from an Aeroderivative Intercooled Gas Turbine. Energy Procedia 2016;101:862–9. https://doi.org/https://doi.org/10.1016/j.egypro.2016.11.109.

[31]   Emadi MA, Chitgar N, Oyewunmi OA, Markides CN. Working-fluid selection and thermoeconomic optimisation of a combined cycle cogeneration dual-loop organic Rankine cycle (ORC) system for solid oxide fuel cell (SOFC) waste-heat recovery. Appl Energy 2020;261:114384. https://doi.org/https://doi.org/10.1016/j.apenergy.2019.114384.

[32]   Lin C-H, Hsu P-P, He Y-L, Shuai Y, Hung T-C, Feng Y-Q, et al. Investigations on experimental performance and system behavior of 10 kW organic Rankine cycle using scroll-type expander for low-grade heat source. Energy 2019;177:94–105. https://doi.org /https://doi .org/10.1016/j.energy.2019.04.015.

[33]   Srinivas T, Gupta AVSSKS, Reddy BV. Thermodynamic modeling and optimization of multi-pressure heat recovery steam generator in combined power cycle. J Sci Ind Res (India) 2008;67:827–34.

[34]   Carapellucci R, Milazzo A. Repowering combined cycle power plants by a modified STIG configuration Energy Convers Manag 2007;48:1590–600.https://doi.org/https: //doi.org/10 .1016/j.enconman.2006.11.024.

[35]   Carapellucci R, Giordano L. Regenerative gas turbines and steam injection for repowering combined cycle power plants: Design and part-load performance. Energy Convers Manag 2021;227:113519. https://doi.org/https://doi.org/10.1016/j.enconman.2020.113519.

[36]   Roy JP, Mishra MK, Misra A. Parametric optimization and performance analysis of a waste heat recovery system using Organic Rankine Cycle. Energy 2010;35:5049–62. https://doi.org/https://doi.org/10.1016/j.energy.2010.08.013.

[37]   Srinivas T, Reddy B. Study on power plants arrangements for integration. Energy Convers Manag 2014;85:7–12. https://doi.org/10.1016/j.enconman.2014.05.057.

[38]   Qiu K, Entchev E. Development of an organic Rankine cycle-based micro combined heat and power system for residential applications. Appl Energy 2020;275:115335. https://doi.org/https://doi.org/10.1016/j.apenergy.2020.115335.

[39]   Köse Ö, Koç Y, Yağlı H. Performance improvement of the bottoming steam Rankine cycle (SRC) and organic Rankine cycle (ORC) systems for a triple combined system using gas turbine (GT) as topping cycle. Energy Convers Manag 2020;211:112745. https://doi.org/10.1016/j.enconman.2020.112745.

[40]   Sachdeva J, Singh O. Thermodynamic analysis of solar powered triple combined Brayton, Rankine and organic Rankine cycle for carbon free power. Renew Energy 2019;139. https://doi.org/10.1016/j.renene.2019.02.128.

[41]   Shamsi SSM, Negash AA, Cho GB, Kim YM. Waste Heat and Water Recovery System Optimization for Flue Gas in Thermal Power Plants. Sustainability 2019;11. https://doi.org/10.3390/su11071881.

[42]   Bălănescu DT, Homutescu VM. Performance analysis of a gas turbine combined cycle power plant with waste heat recovery in Organic Rankine Cycle. Procedia Manuf., vol. 32, Elsevier B.V.; 2019, p. 520–8. https://doi.org/10.1016/j.promfg.2019.02.248.

[43]   Hemadri VB, Subbarao PM V. Thermal integration of reheated organic Rankine cycle (RH-ORC) with gas turbine exhaust for maximum power recovery. Therm Sci Eng Prog 2021;23:100876. https://doi.org/https://doi.org/10.1016/j.tsep.2021.100876.

[44]   Jamil A, Javed A, Wajid A, Zeb MO, Ali M, Khoja AH, et al. Multiparametric optimization for reduced condenser cooling water consumption in a degraded combined cycle gas turbine power plant from a water-energy nexus perspective. Appl Energy 2021;304:117764. https://doi.org/https://doi.org/10.1016/j.apenergy.2021.117764.

Chapter 3 System Description
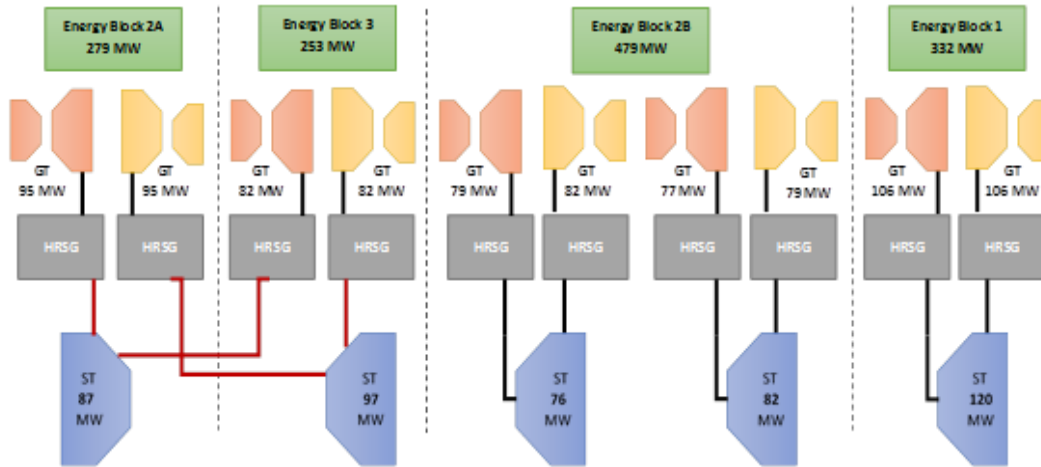
Fig. 3.1 KAPCO power generation facility and the schematic of its different energy generation units with their rated capacity

KAPCO power plant is Pakistan's mega power generation facility with the licensed generation capacity of 1600 MW and a base load generation capacity of 1343 MW. The facility is located in Kot Addu, Sindh and was completed in a tenure of 11 years from 1985-1996 in 5 phases. The latest unit became functional in 1997. The system comprises of 4 energy blocks namely: Energy Block 2A, Energy Block 3, Energy Block 2B and Energy Block 1. The layout of the KAPCO facility is shown in Fig. [3.1]. Energy Block-1 of the KAPCO power generation facility is the latest unit and is the most efficient unit, achieving a net thermal efficiency of 48%. The Energy Block-1 of the KAPCO generation facility comprises of CCGT unit with a 2×1 configuration. The system comprises of 2 GTs coupled with a single ST via 2 HRSGs.

The study is focused on parametric analysis of a TC formed by integrating a Pakistan's based CCGT unit of KAPCO power plant with an ORC unit in the perspective of repowering and

WHR. The thermodynamic performance of the TC is analyzed for the different ORC configurations namely: BORC, SRORC, DRORC, DSRORC. The model of the TC is developed and modeled in a commercial flowsheet software, " Cycle-Tempo". The flowsheet model of the TC modeled in Cycle-Tempo is represented in Fig. [3.7].

3.1 Schematic model of the CCGT unit developed in Cycle-Tempo
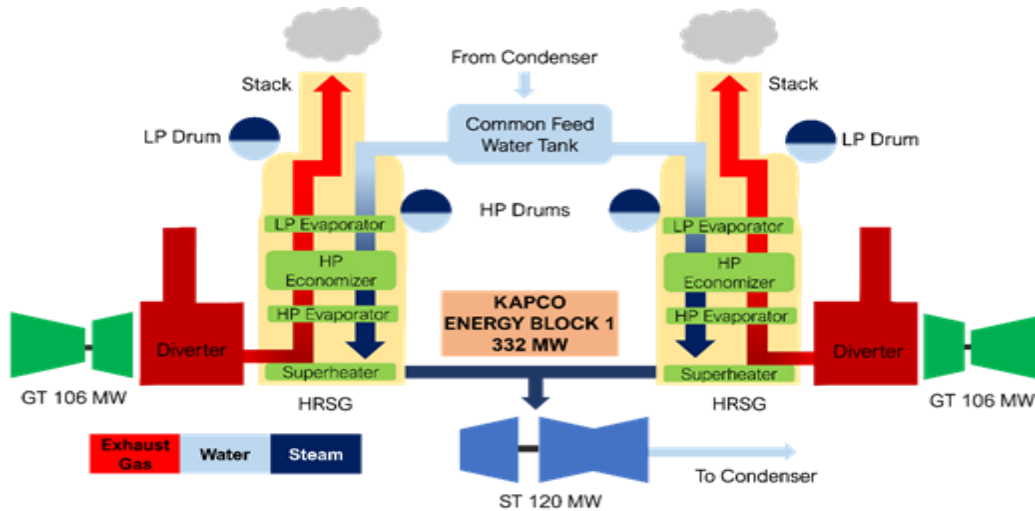
Fig. 3.2 Schematic diagram of the energy block 1 of the KAPCO power generation facility

The CCGT unit of the Energy Block-1 of the KAPCO power plant as shown in Fig.[3.2] comprises of 2 GTs and 2 HRSGs coupled with a single ST, thus forming a 2×1 configuration. The CCGT can run on any of the three fuels that is: natural gas, furnace oil, high-speed diesel. The CCGT unit comprises of two systems of GT cycle namely GT_1 and GT_2 each having a HRSG. Exhaust from GTs is diverted to the respective HRSGs. The HRSGs are of multi-pressure type. The high-pressure loop of each HRSG comprises of an economizer, evaporator and superheater and is used to drive the steam turbine. The low-pressure loop of each HRSG consist of an evaporator, a drum and two pumps. Condensate coming from the condenser is fed to a common feedwater tank via a circulation pump. The feedwater is split into two streams to fed both the HRSGs. Heat is exchanged in the HRSGs to produce superheated steam. Superheated steam coming from both HRSGs is diverted to a common source which then expands through a single ST. The complete detail of the process can be understood through the schematic diagram that is modeled in commercial software Cycle-Tempo.

Fig. 3.3 Flowsheet model of a TC developed in Cycle-Tempo by integrating DSRORC with the CCGT unit of the KAPCO power plant

3.2 ORC Unit

ORC unit is integrated with HRSG of the GT_2 unit parallel to the SRC. ORC recover the heat from the flue gas of CCGT in the primary heat exchanger of ORC. 4 different configurations of ORC namely BORC, SORC, DORC, DSRORC are modelled and integrated with CCGT in Cycle Tempo software individually. Only the DSRORC configuration is being shown integrated with CCGT to form a triple in Fig [3.3]. For all other configurations, the ORC unit can be integrated with CCGT in a similar manner. Table 3.1 shows the essential components and a summary of the processes involved in each ORC component for the different ORC configurations.

Table 3.1 Basic processes involved in each component of the different ORC configuration and their process path.

Component	Process	Process Path			
		BORC	SRORC	DRORC	DSRORC
Pump 1	Pumping	(4r -1r)	$(7_r\text{-}1_r)$	$(10_r\text{-}1_r)$	$(8_r\text{-}1_r)$
Primary heat exchanger	Heat addition	(1r -2r)	$(3_r\text{-}4_r)$	$(5_r\text{-}6_r)$	$(2_r\text{-}3_r)$
Turbine stage 1	Expansion	(2r -3r)	$(4_r\text{-}5_r)$	$(6_r\text{-}7_r)$	$(3_r\text{-}4_r)$
Reheater	Reheating	-	-	-	$(4_r\text{-}5_r)$
Turbine stage 2	Expansion	-	$(5_r\text{-}6_r)$	$(7_r\text{-}8_r)$	$(5_r\text{-}6_r)$
IHE	Pre-heating	-	-	-	$(6_r\text{-}7_r)$
Turbine stage 3	Expansion	-	-	$(8_r\text{-}9_r)$	-
Condenser	Condensation	(3r -4r)	$(6_r\text{-}7_r)$	$(9_r\text{-}10_r)$	$(7_r\text{-}8_r)$
Feedwater heater 1	Regeneration	-	$(5_r\text{-}2_r)$	$(8_r\text{-}2_r)$	-
Pump 2	Pumping	-	$(2_r\text{-}3_r)$	$(2_r\text{-}3_r)$	-
Feedwater heater 2	Regeneration	-	-	$(7_r\text{-}4_r)$	-
Pump 3	Pumping	-	-	$(4_r\text{-}5_r)$	-

3.2.1 BORC
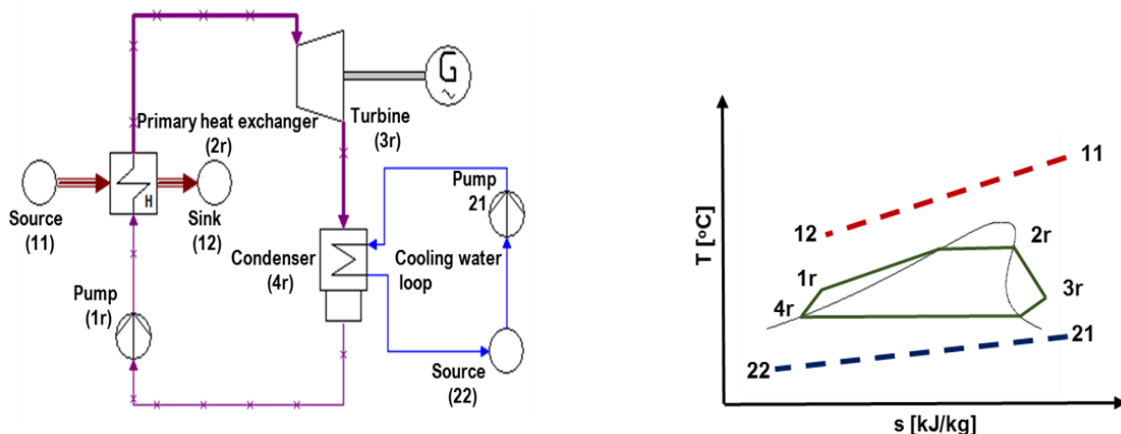
Fig. 3.4 Schematic diagram of a BORC and the respective Ts diagram

23

BORC comprises of a pump, primary heat exchanger, turbine, and a condenser as shown in Fig. [3.4]. The complete process flow of BORC is shown by (1r-4r). The condensed working fluid is pumped to state 1r at primary heat exchanger pressure using pump. The working fluid exchanges heat in the primary heat exchanger and exits as a saturated vapor at state 2r. The high temperature and pressure working fluid is then expanded in a turbine which is connected to a generator. The expanded working fluid then enters the condenser at state 3r. Heat is exchanged between the cooling water and the working fluid. Working fluid exits the condenser as saturated liquid at state 4r.

3.2.2 SRORC

SRORC include pumps, primary heat exchanger, turbine, condenser and an open feedwater heater as shown in Fig [3.5]. The process flow can be described by (1r-7r). Condensed liquid is pumped to the bleeding pressure of working fluid for open feed water heater at state 1r. Heat is exchanged inside the feedwater heater and the pre-heated working fluid exits at state 2r. It is then pumped to the evaporator pressure at state 3r via another pump. The working fluid then exchanges heat with the flue gas in the primary heat exchanger and exits as a saturated vapor at state 4r. The high temperature and pressure working fluid is then expanded through the first stage of turbine before it is bled at state 5r. The remaining mass of working fluid is then expanded through the second stage to the condenser pressure at state 6r. The expanded working fluid is then condensed in a condenser and exits at state 7r.
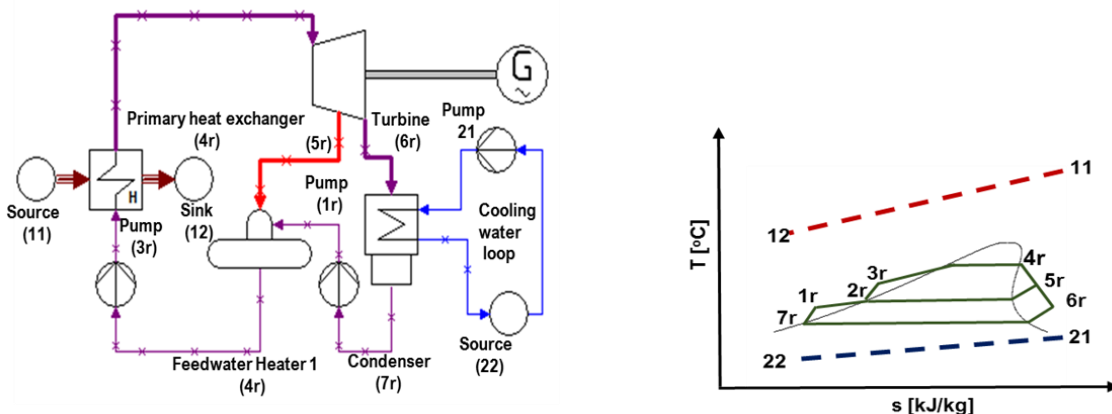
Fig. 3.5 Schematic diagram of a SRORC and the respective Ts diagram

3.2.3 DRORC

DRORC configuration is like SRORC except there are two feedwater heaters and an additional pump as shown in Fig. [3.6]. The cycle can be shown by lines (1r-10r).

The condensate exiting from the condenser is pumped to the 2nd feedwater pressure at state 1r. The high temperature bled working exchanges mixes and exchanges heat with the condensed liquid. The working fluid exits the open feedwater heater at state 2r, and it is pumped to the pressure of feedwater 1 at state 3r. A similar process of heat exchange occurs, and the working
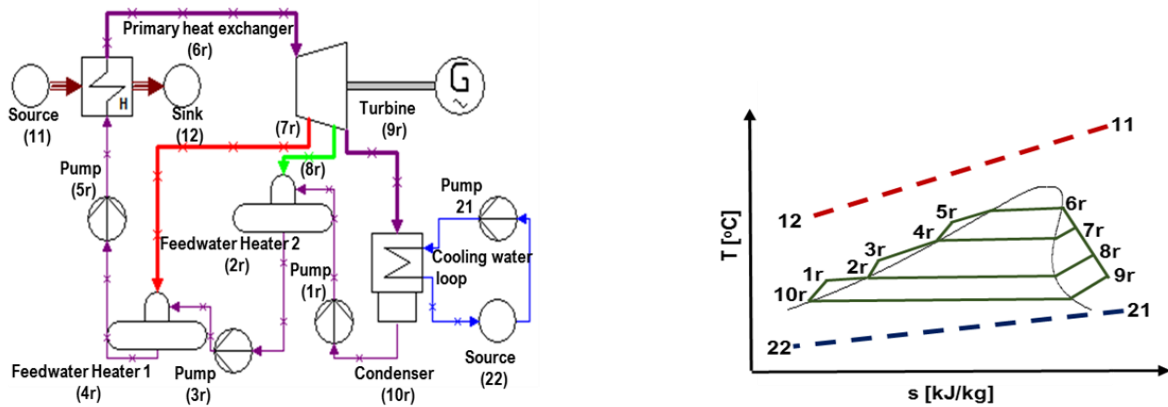
Fig. 3.6 Schematic diagram of a DRORC and the respective Ts diagram

fluid exits the feedwater heater 1 at state 4r. The pre-heated working fluid is then pumped to the evaporator pressure at state 5r. Heat is exchanged between the working fluid and the flue gas in the primary heat exchanger and the saturated vapor is produced at state 6r. It is then expanded through the first stage of the turbine where it is bled at state 7r. The remaining mass of the working fluid is expanded through the second stage until the working fluid is bled again at state 8r. The still available working fluid is then expanded through the last stage of the turbine to state 9r. The working fluid is condensed to state 10r in the condenser.

3.2.4 DSRORC
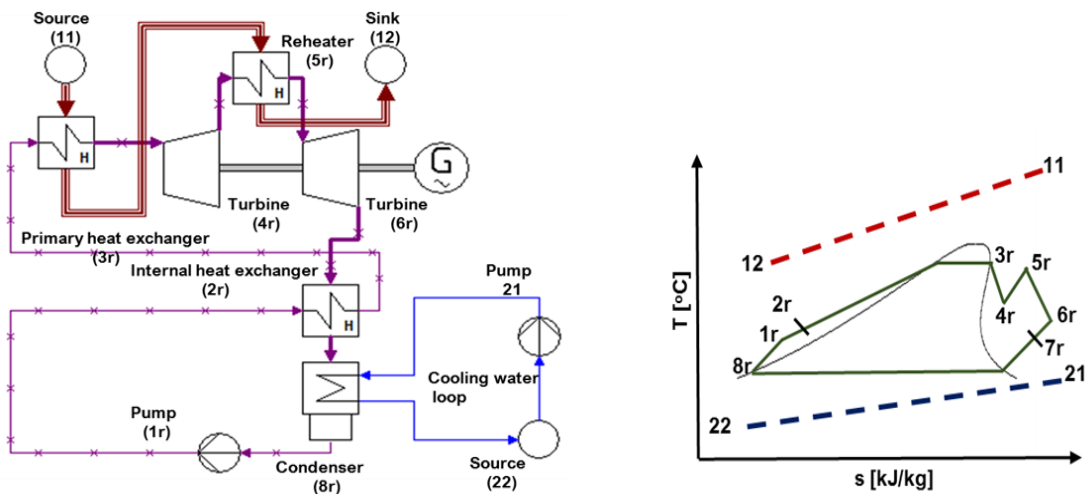
Fig. 3.7 Schematic diagram of a DRORC and the respective Ts diagram

25

DSRORC consists of a pump, primary heat exchanger, turbine, reheater, internal heat exchanger and a condenser as shown in Fig [3.7].

The complete process of DSRORC can be described by line(1r-8r). The condensed working fluid is pumped to its evaporation pressure at state 1r. The working fluid is then passed through an internal heat exchanger where it is pre-heated by exchanging heat with the hot side of working fluid. The pre-heated working fluid enters the primary heat exchanger at state 2r. It exits the primary heat exchanger as a saturated working fluid is then reheat using the recirculated flue gas to state 5r. The reheated working fluid is then expanded via the second stage of the turbine to state 6r. An internal heat exchanger is used to recover the heat of the expanded working fluid to pre-heat the condensed working fluid before entering the primary heat exchanger. The working fluid enters the condenser at state 7r. The working fluid exits the condenser as a condensed liquid at state 8r.

Summary

This chapter elaborates the description of the KAPCO power generation facility particularly the Energy Block-1, the ORC unit and the TC for the different ORC configurations. The Energy Block-1 is a CCGT unit which is a 2×1 power generation facility. The ORC unit which comprises of 4 different configurations is integrated with the CCGT unit to form the TC. SRORC configuration consists of an additional feedwater heater, while DRORC comprises of 2 additional feedwater heaters whereas the DSRORC comprises of a reheater and an internal heat exchanger.

Chapter 4 Modeling of the System

The TC is formed by integrating the CCGT unit and the ORC unit in Cycle-Tempo. The CCGT unit is modeled in Cycle-Tempo using the experimental data obtained for the Energy Block-1 of the KAPCO power plant. The ORC unit which comprises of four different ORC configurations are first modeled in Cycle-Tempo using the exhaust conditions of the CCGT. Each ORC configuration is optimized for the objective function of specific work output. The optimized configurations are integrated with the CCGT unit to form the TC. The ORC unit is integrated with the CCGT unit and the analysis for the TC is carried out using stochastic data obtained of the CCGT to incorporate 24-hour performance variations in net power output.

Cycle-Tempo is a commercial power plant simulation software that applies energy and mass balance equation to the system to calculate unknown enthalpies, mass flows and temperatures. The different components utilized in modeling the TC are mentioned as apparatuses in the Cycle-Tempo software. Depending upon the component, Cycle-Tempo added either a mass or energy equation into the system.

The steps performed in Cycle-Tempo to solve the TC system are summarized as follows.

1.) Development of the flowsheet model of the TC formed by integrating the CCGT and the ORC unit.

2.) Selection of the working fluid based on the fluid library.

3.) Validation of the input data against the fluid properties using a built-in fluid library.

4.) Application of the energy and mass balance equation to calculate unknown mass or enthalpies.

5.) Calculation of temperatures, pressures, and enthalpies for the given input data by adopting an iterative procedure.

6.) Solving the system matrix for calculation of mass flows using Gauss Elimination Method using the enthalpy values of each apparatus calculated in step 5.

7.) Accuracy check is performed using a minimum of 2 iterations; iterations are repeated until the break-off criterion is met.

8.) For the mass flow calculated, unknown pressures, temperatures, enthalpies are calculated for the apparatuses for which EEC is set to be 2.

9.) Calculation of the heat supplied and power output.

10.) Computation of the system thermal efficiency.

11.) TC is simulated iteratively for the 24 hr real-time data. Steps 1-10 are repeated for each simulation.

Table 4.1 Basic input parameters of the CCGT unit of KAPCO power plant

Parameter	Value	Unit
Turbine Inlet Temperature (TIT) of GT_1, GT_2	1042.79	^{o} C
Turbine inlet pressure of GT_1, GT_2	968.0	kPa
Condenser pressure	9.0	kPa
Turbine inlet pressure of ST	4780	kPa
Air mass flow rate for GT_1, GT_2	460, 460	kg/s
Fuel mass flow rate for GT_1, GT_2	9.448, 9.452	kg/s
High pressure steam mass flow rate	127.76	kg/s

4.1 Mathematical Modeling

The mathematical model is based on the calculation of thermodynamic performance of the triple cycle, estimation of specific fuel consumption, fuel savings and specific water consumption.

4.1.1 Triple cycle energy analysis

The Cycle-Tempo has a built-in calculation engine to perform energy analysis of the triple cycle. The net power output of the TC is the sum of the net power output of CCGT and the ORC unit. The net power output of the CCGT is given by:

$$W_{CCGT_{net}} = W_{GTnet_1} + W_{GTnet_2} + W_{STnet} \qquad [1]$$

The thermal efficiency of CCGT is the ratio of net power output of the CCGT unit to the heat input:

$$\eta_{th(CCGT)} = \frac{W_{CCGTnet}}{Q_{CCGT}} \times 100 \qquad [2]$$

Similarly, the thermal efficiency of the ORC unit is given by:

$$\eta_{th(orc)} = \frac{W_{ORCnet}}{Q_{ORC}} \times 100 \qquad\qquad [3]$$

The net power output of the TCPP is the sum of net power output of the CCGT unit and ORC unit.

$$W_{TCnet} = W_{CCGTnet} + W_{ORCnet} \qquad\qquad [4]$$

whereas the thermal efficiency of the TC is given by:

$$\eta_{th(TC)} = \frac{W_{TCnet}}{Q_{TC}} \times 100 \qquad\qquad [5]$$

The input parameters and the flue gas properties used for modeling of the ORC unit are shown in Table 4.1 and 4.2 respectively.

Table 4.2 Flue gas properties and the assumed cycle properties for the ORC unit

Parameters	Value	Unit
Flue gas inlet temperature	168	^{o}C
Flue gas pressure	101.25	kPa
Turbine isentropic efficiency, η_{isen}	0.80	-
Pump isentropic efficiency η_p	0.80	-
Cooling water inlet temperature	10	^{o}C
Mechanical efficiency of turbine, η_{mec}	0.99	-

The different ORC configurations modeled in Cycle-Tempo. The equations applied by the Cycle-Tempo for modeling of each component of the different ORC configurations are listed in in Table 4.3.

4.1.2 Pressure Losses Estimation

As evident from the input parameters described in Table 3, flue gas enters the primary heat exchanger with a very high mass flow rate which results in higher mass flow rate of the working fluid correspondingly, according to the energy balanced applied. Therefore, it is imperative to account for the pressure loses in each major components of the system of both the shell side and the tube side. Pressure loses in the heat exchangers of the system are estimated using the comprehensive design methodology described in Ref [1]. The pressure losses in the different component of the CCGT has been accounted for using the provided experimental data. The pressure losses value for the major components of the ORC unit are usually around 3-8% of the inlet pressure.

Table 4.3 Energy equation employed in each component for the different configurations of ORC

Components	BORC	SRORC	DRORC	DSRORC
Pump 1	$w_p = (h_{1r}-h_{4r})$	$w_p = (1-y)(h_1–h_7)$	$w_p = (1-y-z)(h_{1r}–h_{10r})$	$w_p = (h_{1r} – h_{8r})$
Primary heat exchanger	$q_s = (h_{2r}-h_{1r})$	$q_s = (h_{4r}-h_{3r})$	$q_s = (h_{6r}-h_{5r})$	$q_s = (h_{3r} - h_{2r})$
Turbine Stage 1	$w_t = (h_{2r}-h_{3r})$	$w_t = (h_{4r}-h_{5r})$	$w_t = (h_{6r}-h_{7r})$	$w_t = (h_{3r} – h_{4r})$
Turbine Stage 2	-	$w_t =(1-y)(h_{5r}-h_{6r})$	$w_t = (1-y)(h_{7r}-h_{8r})$	$w_t = (h_{5r} – h_{6r})$
Turbine Stage 3	-	-	$w_t = (1-y-z)(h_{8r}-h_{9r})$	-
Condenser	$q_c = (h_{3r}-h_{4r})$	$q_c = (1-y)(h_{6r}-h_{7r})$	$q_c = (1-y-z)(h_{10r}-h_{9r})$	$q_c = (h_{7r} -h_{8r})$
Reheater	-	-	-	$q_{rh} = (h_{5r} -h_{4r})$
Feed water heater 1	-	$y = \frac{(h2r-h1r)}{(h5r-h1r)}$	$y = \frac{(h4r-h2r)}{(h7r-h2r)}$	-
Feed water heater 2	-	-	$z = \frac{((h3r-h1r)-y(h3r-h1r))}{(h8r-h1r)}$	-
IHE	-	-	-	$\varepsilon = \frac{(h2r-h1r)}{(h6r-h1r)}$
Feed water pump 2	-	$w_p = (h_{3r} – h_{2r})$	$w_p = (1-y)(h_{2r}–h_{3r})$	-

4.1.3 Model for the estimation of specific fuel consumption and annual fuel saving

The SFC of the CCGT unit and the TC can be estimated using the fundamental equation as shown:

$$SFC_{CCGT} = \frac{3600 \times m_{flue}}{W_{CCGT}}$$

[6]

where W_{CCGT} is the net power output of the CCGT unit and m_{flue} is the mass flow rate of the flue gas which is calculated using the equation:

$$m_{flue} = f \times m_a$$

[7]

Here f is the air to fuel ratio.

Similarly specific fuel consumption of the TC is calculated using:

$$SFC_{TC} = \frac{3600 \times m_{flue}}{W_{TC}}$$

[7]

where W_{TC} is the net power output of the TC.

The fuel saved annually can be calculated as shown:

$$AFS_{TC} = (SFC_{CCGT} - SFC_{TC}) \times W_{CCGT} \times \tau$$

[8]

where AFS_{TC} represents the fuel saved annually and τ is the no of operating hrs over the year.

31

$$\text{AFSC}_{\text{TC}} = \left(\frac{\text{AFS}_{\text{TC}} \times \text{HHV}}{3.6 \times 10^6} \right) \times \text{PF} \qquad [9]$$

where HHV is the High-Heating Value of the fuel and PF is the price of the fuel in dollars per MWh. The model used for estimation of AFS and AFSC can be found in Ref [2].

4.1.4 Model for the calculation of SWC

A generic model adopted to estimate the Specific Water Consumption (SWC) of the CCGT unit and the corresponding TC unit can be found in Ref [3]. The waste utilized in any powerplant is given by:

$$\text{SWC} = A(\text{HR} - B) + C \qquad [10]$$

where B (kJ/kWh) represents the heat that is converted into electric power and utilized in other processes of the powerplant except the cooling mechanism as shown by:

$$B = Q_{\text{elec}} + Q_{\text{flue}} \qquad [11]$$

where Q_{elec} represents the heat content of electricity and Q_{flue} is the heat that is rejected in the flue gas. The rejected heat in the flue gas consists of the sensible and latent part as shown by:

$$Q_{\text{sen}} = m_{\text{flue}} c_{\text{p(flue)}} (\Delta T) \qquad [12]$$

where m_{flue} is the mass flow rate of the flue gas, c_{flue} is the specific heat of the flue gas and ΔT represents the change in temperature of the flue gas.

$$Q_{\text{lat}} = m_{\text{flue}} h_{\text{fg}} \qquad [13]$$

where h_{fg} represents the latent heat of vaporization of the flue gas.

HR represents the heat rate of the power plant and can be found using:

$$\text{HR} = m_{\text{flue}} (h_{\text{in}} - h_{\text{out}}) \qquad [14]$$

where h_{in} represents the enthalpy of the flue gas at the inlet of the HRSG and h_{out} is the enthalpy of the flue gas at the exit of the HRSG.

The term (HR-B) quantifies the amount of heat that is rejected in the cooling mechanism.

The term 'A' represents the water consumed or withdrawn per unit of waste heat that is rejected.

It is given by:

$$A_{CTW} = \frac{(1-k_{sen})}{\rho_w h_{fg}} \left(1 + \frac{1}{n_{cc}-1}\right) \qquad [15]$$

This represents the water withdrawn from the cooling tower for evaporative type cooling where k_{sen} is the fraction of the heat load, n_{cc} is the number of cycles of the concentration, ρ_w is the density of the water.

The water consumed is given by:

$$A_{CTC} = \frac{(1-k_{sen})}{\rho_w h_{fgw}} \left(1 + \frac{1-k_{bd}}{n_{cc}-1}\right) \qquad [16]$$

An additional term in this equation is k_{bd} which represents the fraction of the blowdown discharged to the watershed. In this analysis A_{CTW} is assumed to be equal to the A_{CTC} for the evaporative cooling system since the main mechanism of cooling is evaporative.

C represent the water required in other processes of the thermal power plant. The basic input parameters required for the estimation of SFC, AFS, AFSC and SWC are tabulated in Table 4.4.

Table 4.4 Input parameters for the calculation of SFC, AFS, AFSC and SWC

Parameter	Value	Unit
Air to fuel ratio, f	0.019	-
Number of operating hours, τ	8760	hr
Price of the fuel, PF	47	$/MWh
Heat content of electricity, Q_{elec}	3600	kJ/kWh
Number of cycles of concentration ,n_{cc}	20	-
Fraction of the heat load consumed for sensible heat transfer, k_{sen}	0.15	-
Water required in other processes of a thermal power plant, C	0.02	m^3/MWh

4.1.5 Working fluids

The different working fluids considered for modeling of an ORC unit can be classified as dry fluids, wet fluids and isentropic fluids. Dry working fluids exits in superheated state after expansion and have a positive slope [4]. On the other hand wet fluids have negative slope while isentropic fluids have infinite slope [5]. R245fa , R113 and R141b are the working fluids considered in this study. The basic properties of these working fluids are shown in Table 4.5 as found in Ref [6].

33

Table 4.5 Basic thermodynamic properties of the selected working fluids

Working fluid	P_{cri} [kPa]	T_{cri} [°C]	M [kg/kmol]	Safety level	ODP	GWP	Fluid Type
R245fa	3640	154.05	134.05	B1	0	950	Dry
R113	3392	214.06	187.38	-	0.9	6130	Isentropic
R141b	4460	206.81	116.95	A1	0.086	700	Isentropic

4.2 Validation of the model

It is necessary to validate the model of the CCGT unit of the KAPCO power plant before integrating it with the different configurations of ORC. A good accord is seen between the calculated and the observed values for the CCGT unit, as shown in Table 4.6.

Table 4.6 Model validation of the CCGT unit for the calculated and observed values for the designed case.

Cycle Parameter	Calculated Value	Observed Value
GT_1 and GT_2 Power Output (MW)	124.42	125.14
ST Power Output (MW)	149.35	148.03
Net Thermal Efficiency, η_{lth} (%)	45.13	46.08
Condenser Duty (MW)	271.23	271.47
Condenser Cooling flow rate (kg/s)	5650	5650.10

4.3 Optimization methodology

Each configuration of the ORC unit is optimized before integrating with the CCGT unit. With the objective function of specific work output, each configuration of ORC is optimized for at least two input variables. For BORC, turbine inlet pressure and inlet temperature are selected as the input variables. For SRORC, the bleeding pressure of the 1st stage of the turbine along with the turbine inlet pressure is selected as the input variables. Turbine inlet pressure and first and second stage bleeding pressure of the turbine are selected as input variables for DRORC. For DSRORC, turbine inlet pressure and the stage pressure ratio are selected as the input variable with a constrain that pinch point temperature difference (PPTD) should be maintained at 5°C at least between the recirculated flue gas and the reheated working fluid. For each configuration, the turbine inlet temperature is varied between 40°C to a minimum of 7°C (PPTD) for the selected heat source temperature, and an array of turbine inlet and corresponding pressure is generated. A code is developed in MATLAB, and the Cycle-Tempo calculation engine is run in batch mode for the optimization.

Summary

This chapter summarizes the basics of how Cycle-Tempo works in performing the thermodynamic analysis of the different models. The mathematical model for calculating the thermodynamic work output, thermal efficiency , specific fuel consumption and specific water consumption is also elaborated in this section. The optimization scheme is also explained in detail highlighting how different input variables are selected. The model of CCGT for the given data is also validated in this section. The models defined in this section forms the basis of the results discussed in chapter 5.

References

[1]   Towler G, Sinnott R, editors. No Title. Chem. Eng. Des. (Second Ed. Second Edi, Boston:Butterworth-Heinemann;2013,p.1271–303.https://doi.org/https://doi.org/10.1016/B9 78-0-08-096659-5.00036-5.

[2]   Bălănescu DT, Homutescu VM. Performance analysis of a gas turbine combined cycle power plant with waste heat recovery in Organic Rankine Cycle. Procedia Manuf., vol. 32, Elsevier B.V.; 2019, p. 520–8. https://doi.org/10.1016/j.promfg.2019.02.248.

[3]   Delgado A, Herzog H. A simple model to help understand water use at power plants: Working Paper [online] 2012.

[4]   Zhang X, Zhang Y, Wang J. New classification of dry and isentropic working fluids and a method used to determine their optimal or worst condensation temperature used in ORC:Energy 2020;201:117722. https://doi.org/https://doi.org/10.1016/j.energy.2020.117722.

[5]   White JA, Velasco S.Characterizing wet and dry fluids in temperature-entropy diagrams. Energy 2018;154:26976. https://doi.org/https://doi.org/10.1016 /j.energy.2018.04 .105.

[6]   Xi H, Li M-J, Xu C, He Y-L. Parametric optimization of regenerative organic Rankine cycle (ORC) for low grade waste heat recovery using genetic algorithm. Energy 2013;58:473–82. https://doi.org/https://doi.org/10.1016/j.energy.2013.06.039.

Chapter 5 Results and Discussion

The DSRORC configuration is optimized and compared with the standard ORC configurations, namely BORC, SRORC, and DRORC, for the optimal thermodynamic parameters. Each parametrically optimized ORC configuration is integrated with the CCGT model developed in Cycle-Tempo software to form a triple cycle. The thermodynamic performance of the triple cycle is analyzed for each ORC configuration for the working fluid R245fa, R141b, and R113.

5.1 Comparative analysis of each standalone ORC configuration for the optimized thermodynamic parameters

Before integrating each ORC, the configuration is optimized for the objective function of specific work output. The optimized thermodynamic parameters for each ORC configuration are enumerated in Table [5.1-5.4].

Table 5.1 Optimal performance parameters of standalone BORC configuration for the different working fluids

Optimal parameters	R245fa	R113	R141b
Turbine inlet pressure (kPa)	2577.3	802.4	1255.0
Condenser pressure(kPa)	177.79	54.37	94.24
TIT (˚C)	135	128	130
Specific work output (kJ/kg)	34.09	28.77	42.36
Specific heat input (kJ/kg)	249.08	206.21	281.43
Mass flow rate (kg/s)	118.5	117.3	107.8
Thermal efficiency, η_{th} (%)	13.68	13.95	15.05

Results of the optimized configurations of ORC indicate that standalone DSRORC configuration outperforms other configurations in terms of specific work output, whereas standalone DRORC configuration achieves the highest thermal efficiency for all the working fluid considered. R141b is the best performing fluid in terms of specific work output and thermal efficiency for all the considered configurations. The DSRORC produces a specific work output of 48.78 kJ/kg for the working fluid R141b, whereas the DRORC configuration achieves the maximum thermal efficiency of 17.63% for the working fluid R141b. The average relative increase in specific work output for all the considered working fluid while switching from BORC to DSRORC is 12.34%, whereas conversion from SRORC and DRORC to DSRORC results in an increase of 21.45% and 34.53% in the specific work output, respectively.

Table 5.2 Optimal performance parameters of standalone SRORC configuration for the different working fluids

Optimal parameters	R245fa	R113	R141b
Turbine inlet pressure (kPa)	2651.0	835.2	1303.3
Condenser pressure(kPa)	177.79	54.37	94.24
Bleeding pressure (kPa)	662.7	208.7	325.8
Mass fraction of working fluid from 1st stage	0.2296	0.1819	0.1806
TIT (˚C)	136.5	130.0	132.0
Specific work output (kJ/kg)	29.55	27.34	40.43
Specific heat input (kJ/kg)	195.27	172.33	238.76
Mass flow rate (kg/s)	115.7	111.1	103.6
Thermal efficiency, η_{th} (%)	15.13	15.86	16.93

Table 5.3 Optimal performance parameters of standalone DRORC configuration for the different working fluids

Optimal parameters	R245fa	R113	R141b
Turbine inlet pressure (kPa)	2625.0	851.9	1279.0
Condenser pressure (kPa)	177.79	54.37	94.25
Bleeding pressure stage 1 (kPa)	1050.0	425.9	634.9
Mass fraction of working fluid from 1st stage	0.1551	0.1687	0.1513
Bleeding pressure stage 2 (kPa)	656.66	203.97	319.75
Mass fraction of working fluid from 2nd stage	0.1945	0.1607	0.1471
TIT (˚C)	136.00	128.78	131.00
Specific work output (kJ/kg)	26.70	24.66	36.50
Specific heat input (kJ/kg)	161.32	143.77	207.04
Mass flow rate (kg/s)	105.1	102.5	100.3
Thermal efficiency, η_{th} (%)	16.55	17.15	17.63

Table 5.4 Optimal performance parameters of standalone DSRORC configuration for the different working fluids

Optimal parameters	R245fa	R113	R141b
Turbine inlet pressure (kPa)	2577.3	802.4	1255.0
Condenser pressure (kPa)	177.79	54.37	94.24
TIT (˚C)	135	128	130
Stage 1 pressure ratio, r_1	2.87	3.93	2.84
Reheating pressure (kPa)	897.0	204.0	442.5
Degree of reheat (˚C)	25.03	29.80	33.80
Specific work output (kJ/kg)	37.49	31.93	48.78
Net specific heat input (kJ/kg)	233.63	186.77	280.10
Mass flow rate (kg/s)	116.3	112.8	105.4
Thermal efficiency, η_{th} (%)	16.05	17.10	17.42

5.2 Impact of stage pressure ratio and evaporator pressure on the thermodynamic performance of a double stage reheated standalone ORC configuration
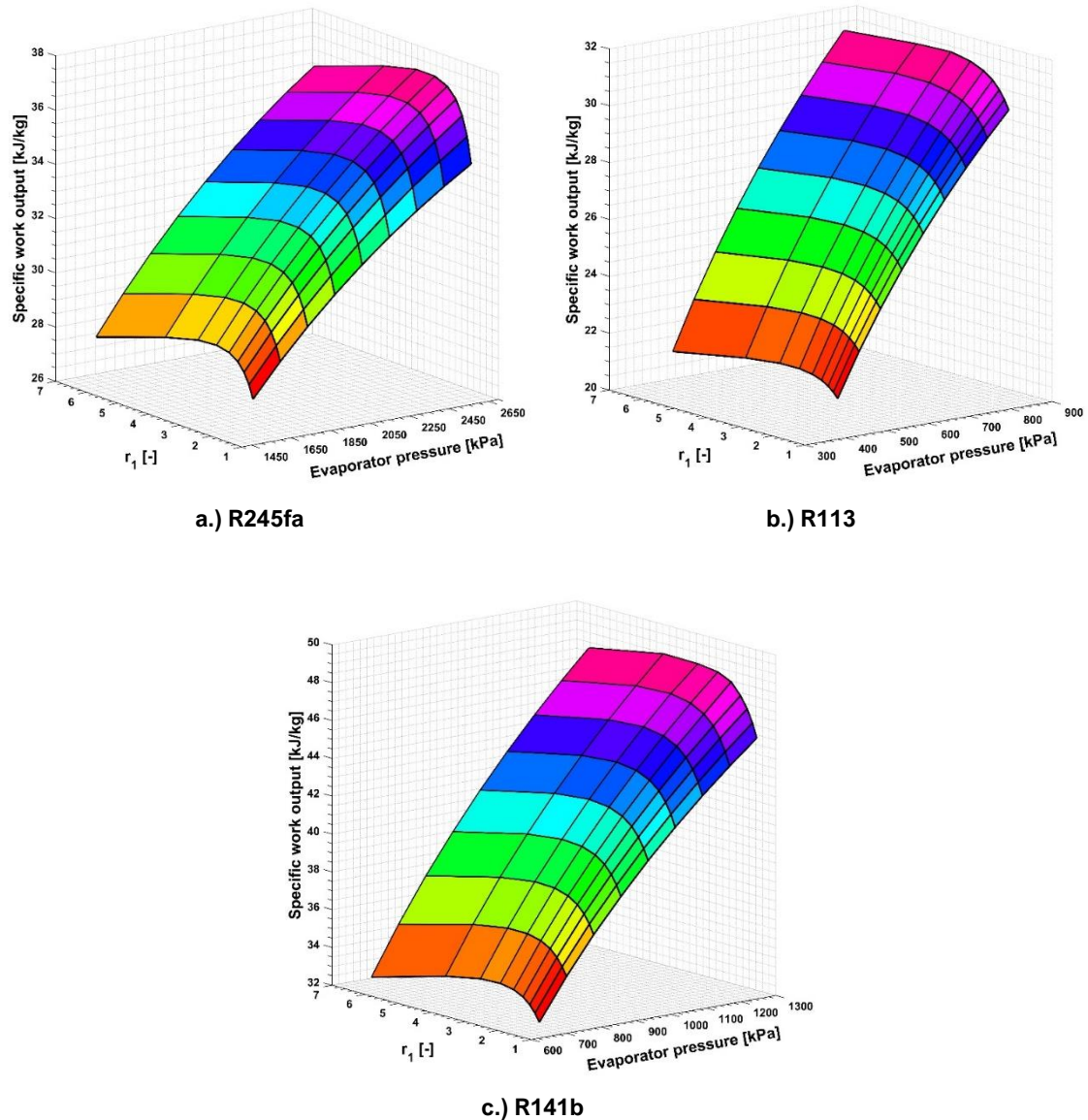

a.) R245fa

b.) R113

c.) R141b

Fig. 5.1 Effect of stage pressure ratio (r_1) and evaporator pressure on the specific work output of the DSRORC for the working fluid (a) R245fa (b) R113 (c) R141b

Evaporator pressure and Stage Pressure Ratio (r_1) are considered as the decision variable in the parametric study of DSRORC. Figure 5.1 demonstrates the effect of r_1 and the evaporator pressure on the specific work output of a DSRORC configuration for the working fluids considered in this study. It is seen that specific work output increases for the increase in
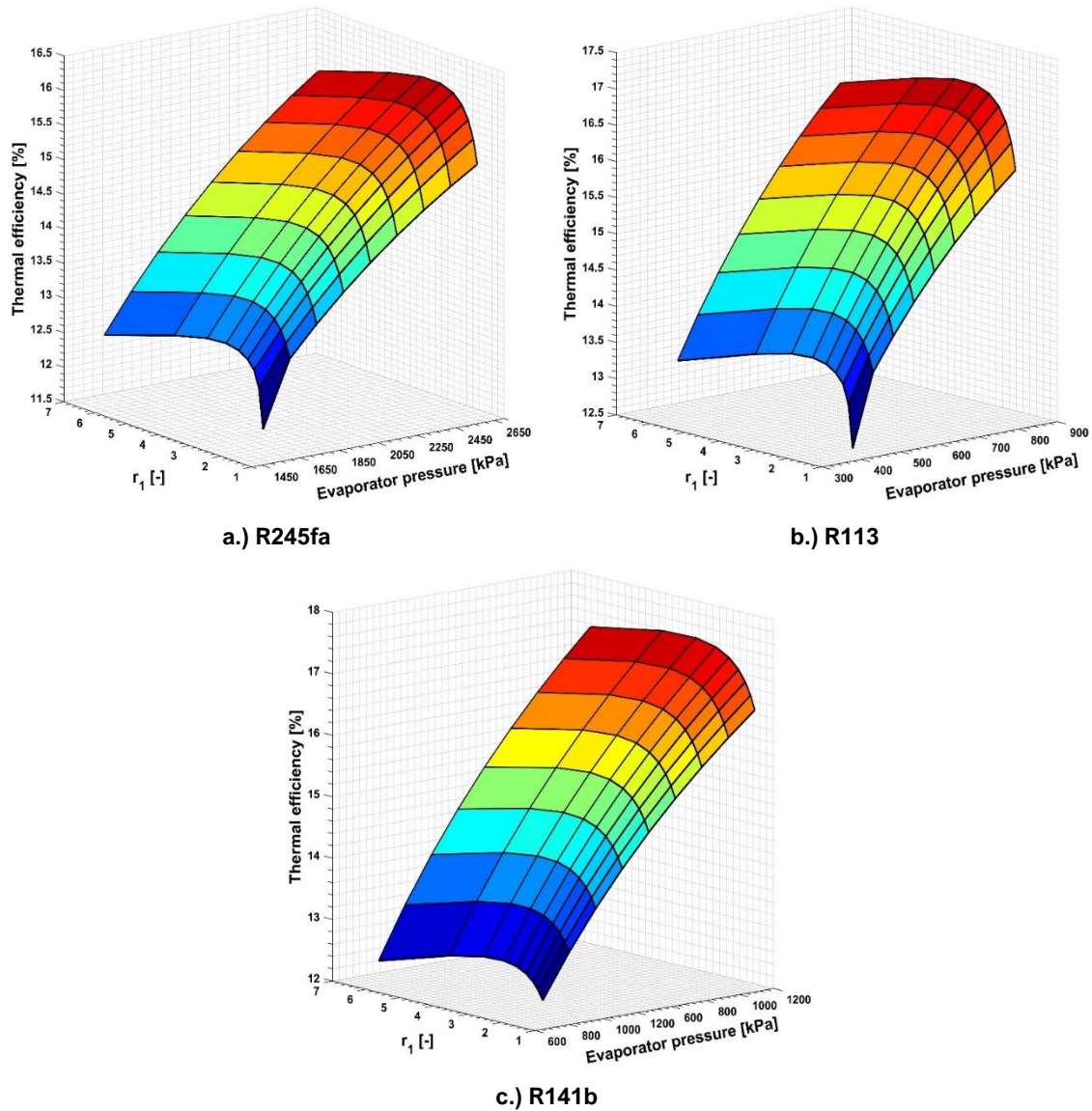
Fig. 5.2 Effect of stage pressure ratio (r_1) and evaporator pressure on the thermal efficiency of a DSRORC for the working fluid (a) R245fa (b) R113 (c) R141b

evaporator pressure for a fixed value of condenser pressure. For a given evaporator pressure, the specific work output of a DSRORC configuration is sensitive to r_1, and the specific work output is maximized for a certain value of r_1, after which it drops. R141b is the best-performing fluid in the perspective of specific work output, followed by R245fa and R113, respectively. A maximum of 48.78 kJ/kg specific work output is achieved by R141b for the evaporator pressure of 1255 kPa and r_1 of 2.84. A similar trend is found for all the working fluids considered in this analysis. R245fa reaches a maximum specific work output of 37.49 kJ/kg for the evaporator pressure of 2577.3 kPa and r_1 of 2.87. R113 achieves a specific work output of 31.93 kJ/kg for the evaporator pressure of 802.39 kPa and r_1 of 3.93.

Figure 5.2 demonstrates the effect of r_1 and evaporator pressure on the thermal efficiency of a DSRORC configuration of ORC for the working fluid R245fa, R113, and R141b, respectively. It is observed that for the given range of evaporator pressure, the thermal efficiency of the DSRORC increases with the increase in evaporator pressure for each working fluid. For a specific evaporator pressure, the thermal efficiency peaks for a particular value of r_1 and then drops because of the drop in specific work output and increased heat load in the reheater. Among the different working fluids considered, R141b is the best-performing fluid and achieves a thermal efficiency of 17.42% for r_1 equal to 2.84, whereas R245fa reaches a thermal efficiency of 16.05% for r_1 equal to 2.87. R113 shows intermediate performance achieving a thermal efficiency of 17.10% for r_1, equal to 3.93. The trend suggests that working fluids like R141b and R113 with higher critical temperatures result in higher thermal efficiency. A Similar trend is observed in Ref [1].

5.3 24-hour performance analysis of the triple cycle for each ORC configuration in perspective of repowering

The net power output of the CCGT unit and the TC for each configuration of the ORC over 24 hours of the day is presented in Fig. [5.3]. 24-hour diurnal data of the CCGT unit indicates that the power output of the CCGT varies over 24-hours of the day, producing a maximum output of 372 MW during 5:00-7:00 hours and reaches a minimum of 355 MW during 13:00-14:00 hours of the day, representing a drop of 17 MW from the peak performance. Integration of the ORC unit with the CCGT results in enhanced power output. Among the different configurations considered, the DSRORC configuration results in maximum enhancement of net power output due to reheating, whereas R141b outperforms other working fluids for all the configurations considered.TC for the BORC configuration exhibits power output comparable to the DSRORC configuration due to the high mass flow rate. On the other hand, TC for SRORC and DRORC configuration results in reduced power output due to lower specific work output and lower working fluid mass flow rate. TC exhibits a trend comparable to the CCGT unit during 24-hours of the day, producing peak power output during 5:00-7:00 hours and reaching minimum power output during 13:00-14:00 hours of the day. During peak performance, TC for the DSRORC exhibits the highest power output of 377.53 MW for the working fluid R141b representing an average increase of 1.37% in the net power output of the CCGT. DRORC configuration results in the slightest enhancement of the net power output of the CCGT. TC for the DRORC configuration results in a minimum power output of 374.53

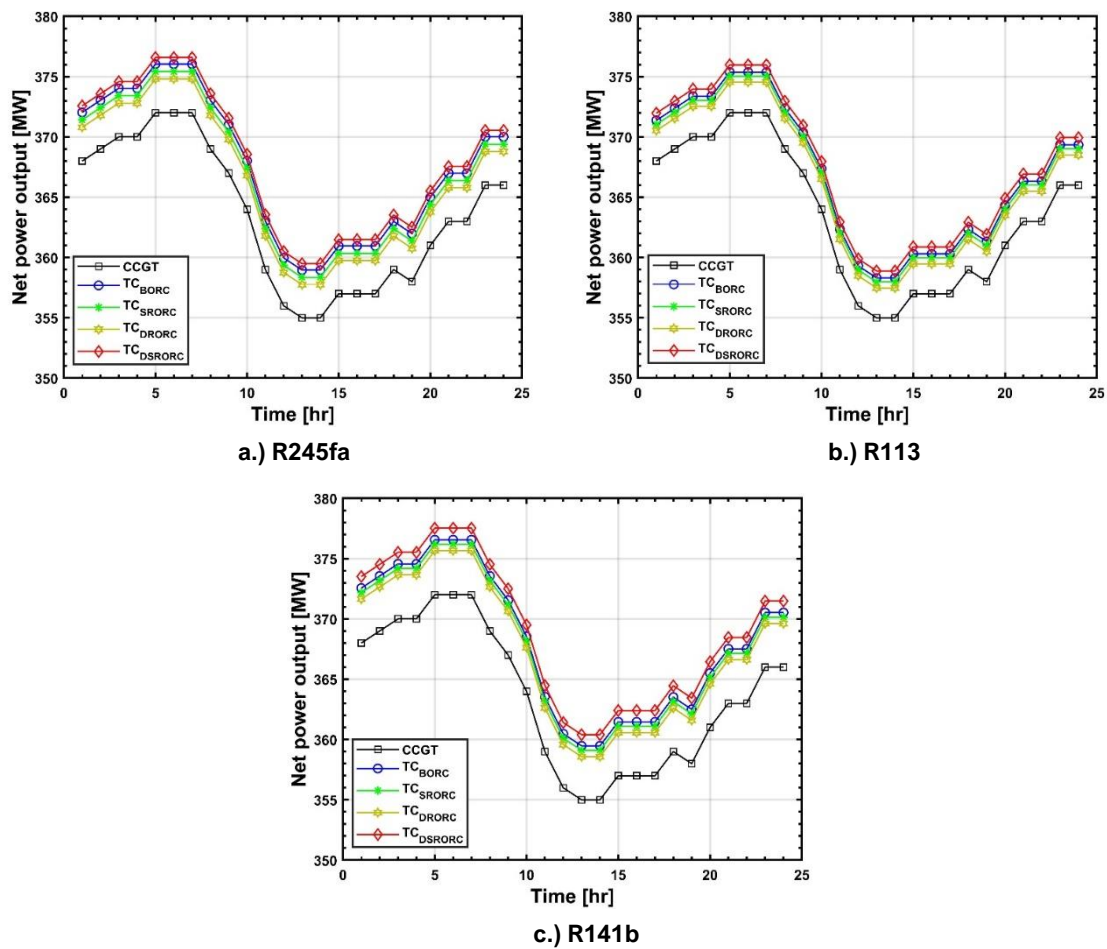MW during peak performance, representing an average increase of 0.55% only in net power output.

Fig. 5.3 24-hour performance analysis of the TC for the different integrated ORC configurations using diurnal data of the CCGT unit for the working fluids (a) R245fa (b) R113 (c) R141b

5.4 Overall effect of integrating different ORC configurations on the average net power output and the thermal efficiency of the CCGT unit

Figure 5.4 shows the average net power output added by integrating each ORC configuration with the CCGT unit for the considered working fluids. DSRORC outperforms other configurations for the net power output, whereas R141b is the best working fluid for net power output. The order of the net power output added as evident in Fig. [5.4] is DSRORC > BORC > SRORC > DRORC, whereas for the working fluids, the order is as R141b > R245fa > R113. DSRORC configuration adds an average of 5.10 MW of net power output for the working fluid R141b, while DRORC configuration adds a minimum net power output of 2.50 MW for the

working fluid R113. DSRORC outperforms other configurations for the net power output because of its high specific work output due to reheating and high mass flow rate requirement.
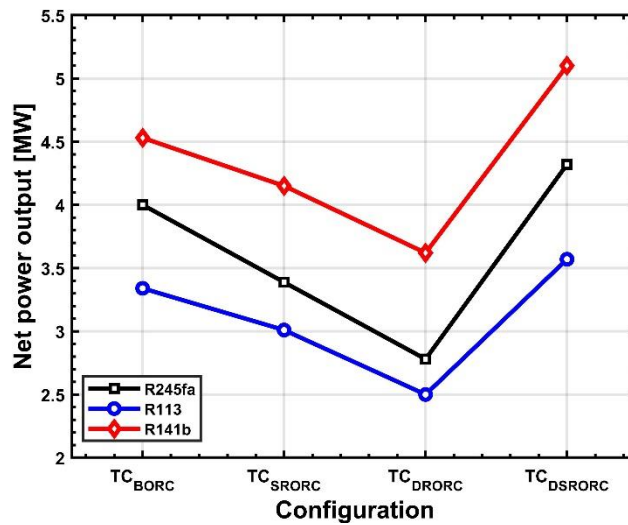

Fig. 5.4 Average net power output added by integrating different ORC configurations with the CCGT unit for the selected working fluids

The overall impact of integrating different configurations of the ORC unit on the CCGT unit in terms of thermal efficiency is represented in Fig. [5.5]. It is seen that the thermal efficiency of the TC is higher than that of a standalone CCGT. The order of the thermal efficiency of the TC for each integrated ORC configuration is as DSRORC > BORC > SRORC > DRORC. R141b outperforms other working fluids for each ORC configuration in terms of thermal efficiency. A maximum of 1.40% relative increase in thermal efficiency is observed for the DSRORC configuration using R141b as the working fluid. A minimum of 0.68% increase in thermal efficiency is observed for the TC when the CCGT unit is integrated with the DRORC configuration of the ORC unit for the working fluid R113. For a standalone configuration, SRORC and DRORC exhibit higher thermal efficiency than the BORC, whereas, for the integrated configurations to form the TC, BORC outperforms SRORC and DRORC in terms of thermal efficiency because the calculation engine of the Cycle-Tempo uses the LHV of the fuel and the net power output to compute the thermal efficiency. Since the ORC unit utilizes the waste heat only, the net power output is the only parameter that affects the thermal efficiency, which is higher in the case of a BORC configuration than the integrated SRORC and DRORC configuration.
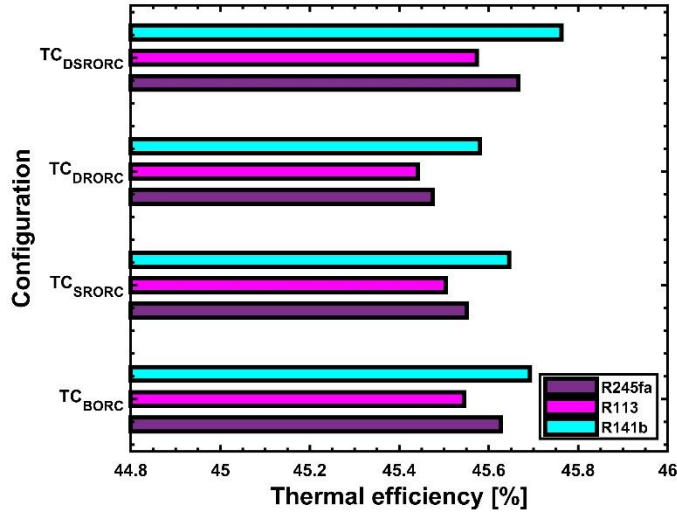
Fig. 5.5 Average thermal efficiency of the TC for each integrated ORC configuration using the working fluids (a) R245fa (b) R113 (c) R141b

5.5 Analysis of the triple cycle for each ORC configuration in terms of mass flow rate and outlet temperature of the flue gas

The effect of each integrated configuration of the ORC unit on the mass flow rate of the working fluid and outlet temperature of the flue gas for the working fluid R245fa, R113, and R141b is presented in Fig. [5.6]. The analysis of the TC formed by integrating different ORC configurations with the CCGT unit indicates that a low mass flow rate is required by the SRORC and DRORC configuration compared to BORC and DSRORC configuration. The SRORC and DRORC configuration have lower primary heat exchanger loads, which
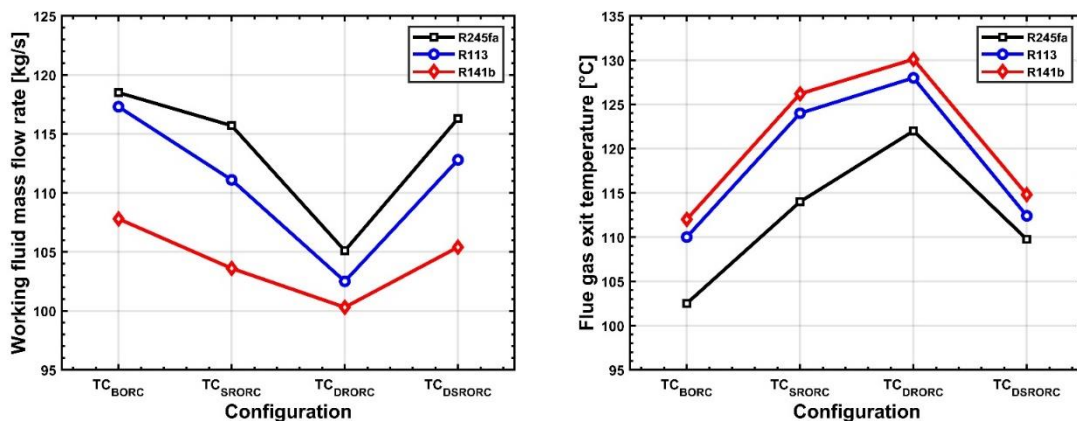

Fig. 5.6 Effect of integrating different ORC configurations with the CCGT unit to form TC on the mass flow rate of the working fluid and flue gas exit temperature

leads to lower mass flow rates. A similar trend can be observed for the SRORC and DRORC configuration in Ref [2]. Between BORC and DSRORC, a lower mass flow rate is required by DSRORC configuration because to reheat the expanded working fluid to the acceptable temperature, the recirculated flue gas temperature must be high enough so that the temperature profiles for the high and low end of the reheater does not cross. Therefore, a slight increase in exit temperature of the flue gas from the primary heat exchanger is observed, leading to the lower mass flow rate of the working fluid according to the mass equation applied by Cycle-Tempo. A maximum flow rate of 118.5 kg/s is required by BORC configuration for the working fluid R245fa, while a minimum mass flow rate of 100.3 kg/s is found for the DRORC configuration using R141b as the working fluid. This concept can be extended to investigate the effect of each configuration on the outlet temperature of the flue gas. Cycle-Tempo applies energy balance on the primary heat exchanger to calculate the outlet temperature of the flue gas. Due to lower evaporator heat load, SRORC and DRORC configurations have higher flue gas exit temperatures than BORC and DSRORC configurations. BORC results in the lowest outlet temperature of the flue gas owing to the higher heat load. DSRORC exhibits outlet temperature of the flue gas comparable to BORC configuration because the temperature of the flue gas exiting the primary heat exchanger of a DSRORC configuration is reduced further after exchanging the heat in the reheater. R245fa results in the lowest outlet temperature of 102.5°C of the flue gas for the BORC configuration, whereas R141b results in the highest exit temperature of 130.1°C of the flue gas for the DRORC configuration.

5.6 Analysis of the triple for each ORC configuration in terms of specific fuel consumption and specific water consumption

The SFC, the corresponding fuel saved annually, and the associated cost saved by integrating the different configurations of the ORC unit with the CCGT to form a TC, compared to the standalone CCGT unit, are demonstrated in Fig. [5.7] It is seen that the SFC of the TC for each configuration of the ORC unit is less than the SFC of the standalone CCGT unit. As the DSRORC configuration results in maximum net power output for TC, its SFC is least while the TC for the DRORC configuration results in maximum SFC among the different configurations analyzed.

This trend is exhibited by every working fluid that is considered in this study. It is seen that the integration of the DSRORC configuration with the CCGT unit using R141b as the working fluid results in the least SFC of 0.1709 kg/kWh leading to a corresponding decrease of 1.28%

in SFC compared to the CCGT unit corresponding to an AFS of 5,254,029 kg which leads to a cost of 3,806,981 $ saved annually. R113 results in a SFC of 0.1720 kg/kWh for the DRORC configuration, corresponding to a decrease of 0.64% in SFC. This is equivalent to an AFS of 2,839,704 kg leading to an annual cost saving of 2,057,602 $.
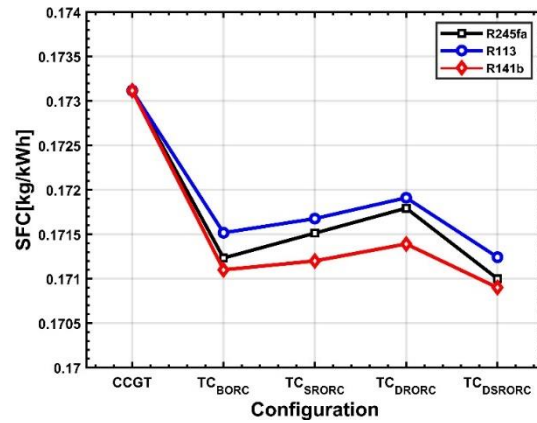
a.) Specific fuel consumed per kWh of power
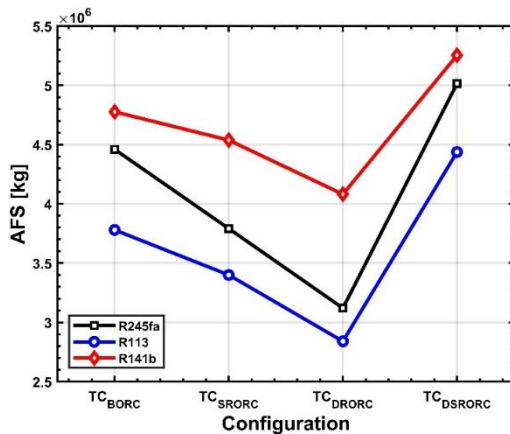
b.) Fuel saved annually
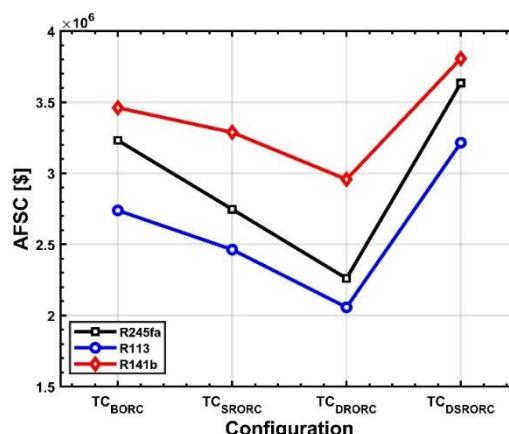
c.) Associated cost saved annually

Fig. 5.7 Effect of integrating different ORC configurations with the CCGT unit to form TC in terms of (a) Specific fuel consumed per kWh of power output (b) Fuel saved annually (c) Associated cost saved annually

Figure 5.8 represents the SWC of the standalone CCGT unit and the TC for each integrated ORC configuration. Integration of the ORC unit with the standalone CCGT unit results in lower SWC than the CCGT power plant because of the additional power output. The water consumption of the ORC unit is negligible compared to the CCGT unit, and therefore it is ignored. For all the considered configurations, the DSRORC configuration of TC results in the least SWC for all the working fluids because the DSRORC configuration results in maximum net power output compared to other ORC configurations. For the different fluids considered, R141b is the best performing fluid. In contrast, the DRORC configuration of the ORC unit

results in maximum SWC among all the configurations analyzed. R141b for the DSRORC configuration yields a minimum SWC of 0.8725 m³/MWh, whereas R113 for the DRORC configuration results in a maximum SWC of 0.8880 m³/MWh.
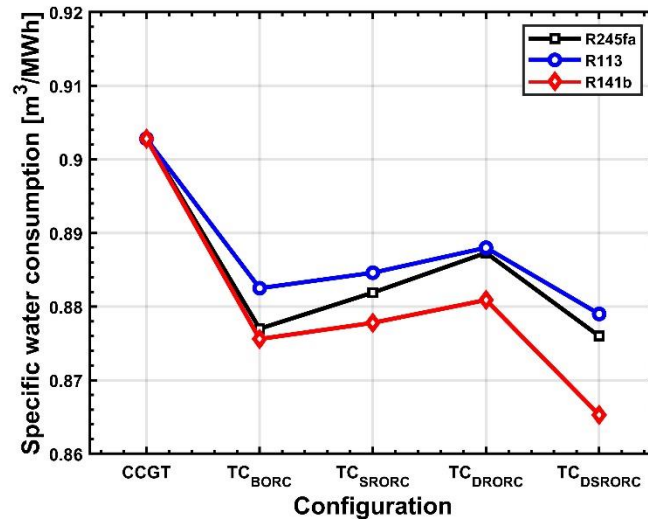

Fig. 5.8 SWC for the different integrated configurations of the ORC unit of TC as compared to the stand-alone CCGT unit for the selected working fluids.

5.7 Waste heat recovered and the reduction in associated emissions by integrating different ORC configurations with the CCGT unit
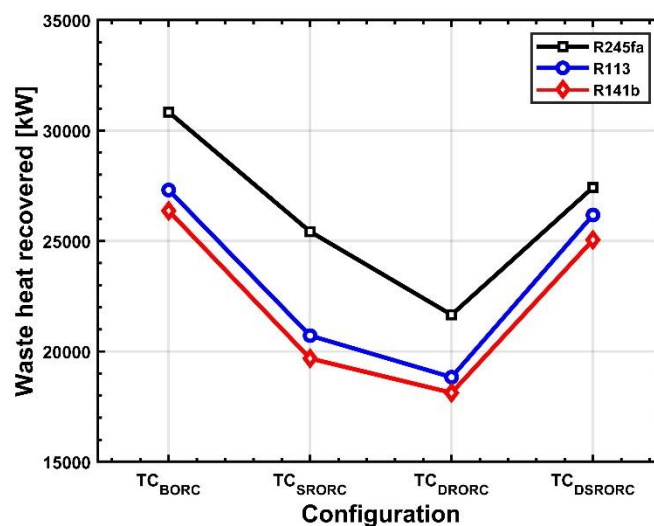

Fig. 5.9 Waste heat recovered by integrating different ORC configurations with the CCGT unit for the selected working fluids.

The waste heat recovered by integrating different configurations of the ORC unit with the CCGT unit to form a triple cycle is shown in Fig. [5.9]. It is seen that the BORC and DSRORC configuration of the ORC unit has exhibited the highest and comparable WHR potential owing to their lower outlet temperature of the flue gas. On the other hand, SRORC and DRORC have lower WHR potential because of lower evaporator loads and correspondingly higher flue gas exit temperature. R245fa has demonstrated the highest WHR potential for all the configurations analyzed. A maximum of 30839.58 kW of waste heat is recovered using R245fa as a working fluid for the BORC configuration of the ORC unit. On the other hand, R141b shows the minimum WHR potential for all the configurations, and a minimum of 18127.1 kW of waste heat is recovered for the DRORC configuration using R141b as the working fluid. For the different configurations considered in this study, R141b results in the lowest mass flow rate, leading to higher flue gas exit temperature according to the energy balance applied by the Cycle-Tempo on the primary heat exchanger thereby, resulting in reduced WHR potential for the working fluid R141b.
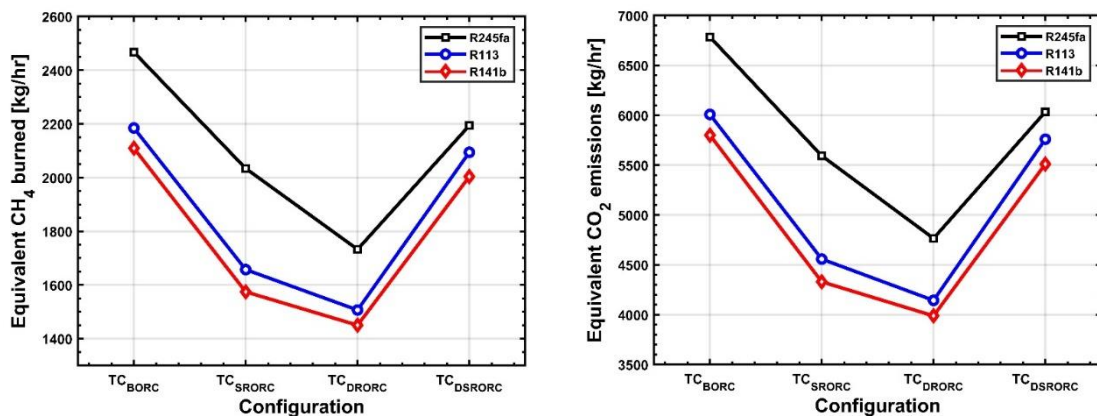

Fig 5.10 Amount of fuel (CH_4) burnt and the CO_2 emissions equivalent to the waste heat recovered for all the integrated configurations of ORC using selected working fluids.

Figure 5.10 quantifies the CH_4 burnt and CO_2 emissions equivalent to the waste heat recovered by integrating different configurations with the CCGT unit using LHV of the fuel provided by Cycle-Tempo and the basic combustion equation. It is seen that the maximum heat recovered by R245fa for the BORC configuration is equivalent to the burning of 2467.2 kg/h of CH_4 that would emit a total of 6784.7 kg/h CO_2 emissions. On the other hand, as discussed earlier, the lowest waste heat recovered for R141b for the DRORC configuration, would be produced if 1450.2 kg/h of CH_4 fuel is burned, causing an equivalent of 3987.9 kg/h CO_2 emissions.

Summary

This chapter explains the result obtained from the mathematical model discussed in chapter 4. Each result is elaborated in the light of thermodynamic principles. It is found out that thermal efficiency and specific work output increases with the increase in evaporator pressure whereas the thermal efficiency and specific work output peaks for a certain value of stage pressure ratio. 24-hour performance variation of the CCGT unit and the TC formed by integrating each ORC configuration is compared and analyzed. It is found out that thermal efficiency and net power output of the TC is more than the CCGT unit. Furthermore, it is found out that the working fluid and configuration of ORC affects the flue gas exit temperature and mass flowrate of the working fluid. SFC and SWC of the TC is much lower than the CCGT unit. The integration of the different ORC configurations with the CCGT unit to form the TC results in lower emissions as well.

References

[1]   Javanshir A, Sarunac N, Razzaghpanah Z. Thermodynamic analysis of a regenerative organic Rankine cycle using dry fluids. Appl Therm Eng 2017;123:852–64. https://doi.org/https://doi.org/10.1016/j.applthermaleng.2017.05.158.

[2]   Xi H, Li M-J, Xu C, He Y-L. Parametric optimization of regenerative organic Rankine cycle (ORC) for low grade waste heat recovery using genetic algorithm. Energy2013;58:473–82. https://doi.org/https://doi.org/10.1016/j.energy.2013.06.039.

Chapter 6 Conclusions and Future Work

In the present study, a newly modified double stage reheated ORC has been optimized for the objective function of specific work output and is compared with other conventional ORC configurations namely, Basic ORC, single stage regenerative ORC and double stage regenerative ORC configuration for the optimal thermodynamic parameters. Three different working fluids R245fa, R113 and R141b are considered in the analysis of the ORC unit. The optimized configurations are integrated with combined cycle gas turbine power plant to form a triple cycle. The thermodynamic performance of the triple cycle is assessed for each configuration in the perspective of waste heat recovery-based repowering, specific fuel consumption, specific water consumption and greenhouse gas emissions.

6.1 Major findings

Following are the major findings of this study:

- Optimization of a standalone double stage reheated ORC has revealed its thermal efficiency and specific work output is sensitive to stage pressure ratio. Thermal efficiency and specific work output increase with the increase in the evaporator pressure for the given range, whereas peak for a particular value of stage pressure after which drop is observed.

- Integration of the ORC unit to recover waste heat from a combined cycle gas turbine has resulted in enhanced power output and thermal efficiency along with reduced specific fuel and specific water consumption and reduced greenhouse gas emissions.

- Mass flow rate of the working fluid of the ORC unit and flue gas exit temperature depends upon the working fluid type and the ORC configuration

- Standalone double stage regenerative ORC achieves the highest thermal efficiency of 17.63% for the working fluid R141b. In contrast double stage reheated ORC configuration achieves the maximum specific work output of 48.78 kJ/kg at a stage pressure ratio of 2.84 for the working fluid R141b.

51

- 24-hour performance variation of the combined cycle gas turbine unit has demonstrated that the net power output of the combined cycle unit of the KAPCO power plant experiences a drop of 17 MW from its peak performance during the 13:00-14:00 hr of the day. The triple cycle for the double stage reheated ORC configuration has resulted in maximum increase of 1.37% in net power output for the working fluid R141b equivalent to 5.10 MW of additional power output.

- Triple cycle for the double stage reheated ORC configuration has outperformed other configurations in terms of thermal efficiency, specific fuel and specific water consumption. The maximum percentage increase in the thermal efficiency of the integrated double stage reheated ORC is found to be 1.40% for the working fluid R141b, whereas the specific fuel and specific water consumption are reduced by 1.5% and 4.1%, respectively.

- The triple cycle for the basic ORC configuration has exhibited the highest waste heat recovery potential. A maximum of 30,840 kW of waste heat is recovered for the working fluid R245fa. The waste heat recovered is equivalent to the burning of 2,467.2 kg/hr of CH_4, leading to 6784.7 kg/hr emissions of CO_2.

- R141b has demonstrated superior thermodynamic performance in terms of specific work output and thermal efficiency whereas, R245fa is weeded out for its higher evaporator load, higher mass flow rate and lower thermal efficiency.

6.2 Future work

After completion of this work, still there are many potential avenues which are available for further research and detailed analysis.

Following are some of the aspects which can be investigated further:

- Dynamic modeling of the CCGT can be done which will provide dynamic input data for modeling of the ORC unit.

- Thermodynamic performance of the zeotropic mixtures can be investigated in modeling of the ORC unit.
- Exergy analysis of the ORC unit for each ORC configuration can be done in order to get better understanding of the triple cycle thermodynamic performance.
- Economic analysis and sizing of the turbomachinery is another potential aspect which shall be further investigated.
- Reheating the working fluid via an external source is also a possibility which needs detailed analysis and research.

Appendix

Publication (Revisions due)

Manuscript Number:	ECM-D-21-05399
Article Type:	Original research paper
Section/Category:	1. Energy Conservation and Efficient Utilization
Keywords:	Combined-cycle gas turbine; waste heat recovery; Organic Rankine cycle; triple-cycle; thermodynamic cycle optimization; specific water consumption
Corresponding Author:	Adeel Javed, PhD National University of Sciences and Technology Islamabad, PAKISTAN
First Author:	Muhammad Reshaeel, MS
Order of Authors:	Muhammad Reshaeel, MS
	Adeel Javed, PhD
	Ahmad Jamil, MS
	Majid Ali, PhD
	Mariam Mahmood, PhD
	Adeel Waqas, PhD
Abstract:	The challenge of meeting ever-expanding energy demand and mitigating climate change requires shifting towards renewable technologies while making existing technologies energy-efficient and environment-friendly. Therefore, this study has considered a combined cycle gas turbine unit as a test case to analyze the effect of integrating different organic Rankine cycle configurations in the perspective of repowering. The study has conducted parametric optimization of a newly modified double stage reheated organic Rankine cycle configuration and its comparison with other conventional configurations of the organic Rankine cycle for optimal thermodynamic parameters using R245fa, R113, and R141b as working fluids. The optimized configurations are integrated with the combined cycle to form a triple cycle using 24-hour diurnal performance data of the combined cycle. It is found that the double stage reheated organic Rankine cycle configuration outperforms other configurations in terms of thermodynamic performance. The integration of the double stage reheated organic Rankine cycle with combined cycle gas turbine has resulted in an additional 5.12 MW of net power output, with a corresponding increase of 1.51% in thermal efficiency and a reduction of 2.70% in specific water consumption. The specific fuel consumption is reduced by 2.49% leading to an annual fuel saving of 7,005,000 kg with an associated annual cost saving of 4,630,000 $. The best waste heat recovery potential is exhibited by the integrated basic organic Rankine cycle configuration for the working fluid R245fa, recovering 29662.49 kW of waste heat, equivalent to the burning of 2135.7 kg/hr of CH_4 and 5873.18 kg/h CO_2 emissions.